

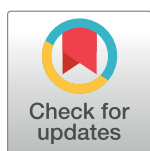
RESEARCH ARTICLE

The Stochastic Early Reaction, Inhibition, and late Action (SERIA) model for antisaccades

Eduardo A. Aponte^{1*}, Dario Schöbi¹, Klaas E. Stephan^{1,2}, Jakob Heinzle^{1*}

1 Translational Neuromodeling Unit, Institute for Biomedical Engineering, University of Zurich & Swiss Institute of Technology Zurich, Zurich, Switzerland, **2** Wellcome Trust Centre for Neuroimaging, University College London, London, United Kingdom

* aponte@biomed.ee.ethz.ch (EAA); heinzle@biomed.ee.ethz.ch (JH)



Abstract

The antisaccade task is a classic paradigm used to study the voluntary control of eye movements. It requires participants to suppress a reactive eye movement to a visual target and to concurrently initiate a saccade in the opposite direction. Although several models have been proposed to explain error rates and reaction times in this task, no formal model comparison has yet been performed. Here, we describe a Bayesian modeling approach to the antisaccade task that allows us to formally compare different models on the basis of their evidence. First, we provide a formal likelihood function of actions (pro- and antisaccades) and reaction times based on previously published models. Second, we introduce the *Stochastic Early Reaction, Inhibition, and late Action model* (SERIA), a novel model postulating two different mechanisms that interact in the antisaccade task: an early GO/NO-GO race decision process and a late GO/GO decision process. Third, we apply these models to a data set from an experiment with three mixed blocks of pro- and antisaccade trials. Bayesian model comparison demonstrates that the SERIA model explains the data better than competing models that do not incorporate a late decision process. Moreover, we show that the early decision process postulated by the SERIA model is, to a large extent, insensitive to the cue presented in a single trial. Finally, we use parameter estimates to demonstrate that changes in reaction time and error rate due to the probability of a trial type (pro- or antisaccade) are best explained by faster or slower inhibition and the probability of generating late voluntary prosaccades.

OPEN ACCESS

Citation: Aponte EA, Schöbi D, Stephan KE, Heinzle J (2017) The Stochastic Early Reaction, Inhibition, and late Action (SERIA) model for antisaccades. *PLoS Comput Biol* 13(8): e1005692. <https://doi.org/10.1371/journal.pcbi.1005692>

Editor: Adrian M. Haith, Johns Hopkins University, UNITED STATES

Received: February 5, 2017

Accepted: July 20, 2017

Published: August 2, 2017

Copyright: © 2017 Aponte et al. This is an open access article distributed under the terms of the [Creative Commons Attribution License](https://creativecommons.org/licenses/by/4.0/), which permits unrestricted use, distribution, and reproduction in any medium, provided the original author and source are credited.

Data Availability Statement: All relevant data are within the paper and its Supporting Information files.

Funding: This work was supported by the René and Susanne Braginsky Foundation (KES) and the University of Zurich. The funders had no role in study design, data collection and analysis, decision to publish, or preparation of the manuscript.

Competing interests: The authors have declared that no competing interests exist.

Author summary

One widely replicated finding in schizophrenia research is that patients tend to make more errors than healthy controls in the antisaccade task, a psychometric paradigm in which participants are required to look in the opposite direction of a visual cue. This deficit has been suggested to be an endophenotype of schizophrenia, as first order relatives of patients tend to show similar but milder deficits. Currently, most models applied to experimental findings in this task are limited to fit average reaction times and error rates. Here, we propose a novel statistical model that fits experimental data from the antisaccade task,

beyond summary statistics. The model is inspired by the hypothesis that antisaccades are the result of several competing decision processes that interact nonlinearly with each other. In applying this model to a relatively large experimental data set, we show that mean reaction times and error rates do not fully reflect the complexity of the processes that are likely to underlie experimental findings. In the future, our model could help to understand the nature of the deficits observed in schizophrenia by providing a statistical tool to study their biological underpinnings.

Introduction

In the antisaccade task ([1]; for reviews, see [2,3]), participants are required to saccade in the contralateral direction of a visual cue. This behavior is thought to require both the inhibition of a reflexive saccadic response towards the cue and the initiation of a voluntary eye movement in the opposite direction. A failure to inhibit the reflexive response leads to an erroneous saccade towards the cue (i.e., a prosaccade), which is often followed by a corrective eye movement in the opposite direction (i.e., an antisaccade). As a probe of inhibitory capacity, the antisaccade task has been widely used to study psychiatric and neurological diseases [3]. Notably, since the initial report [4], studies have consistently found an increased number of errors in patients with schizophrenia when compared to healthy controls, independent of medication and clinical status [5–8]. Moreover, there is evidence that an increased error rate constitutes an endophenotype of schizophrenia, as antisaccade deficits are also present in non-affected, first-degree relatives of diagnosed individuals (for example [5,7]; but for negative findings see for example [9,10]).

Unfortunately, the exact nature of the antisaccade deficits and their biological origin in schizophrenia remain unclear. One path to improve our understanding of these experimental findings is to develop generative models of their putative computational and/or neurophysiological causes [11]. Generative models that capture the entire distribution of responses can reveal features of the data that are not apparent when only considering summary statistics such as mean error rate (ER) and reaction time (RT) [12–15]. Additionally, this type of model can potentially relate behavioral findings in humans to their biological substrate.

Here, we apply a generative modeling approach to the antisaccade task. First, we introduce a novel model of this paradigm based on previous proposals [16–20]. For this, we formalize the ideas introduced by Noorani and Carpenter [17] and extend them into what we refer to as the *Stochastic Early Reaction, Inhibition and late Action* (SERIA) model. Second, we apply both models to an experimental data set of three mixed blocks of pro- and antisaccades trials with different trial type probability. More specifically, we compare several models using Bayesian model comparison. Third, we use the parameter estimates from the best model to investigate the effects of our experimental manipulation. We found that there was positive evidence in favor of the SERIA model when compared to our formalization of the model proposed in [17]. Moreover, the parameters estimated through model inversion revealed the complexity of the decision processes underlying the antisaccade task that is not obvious from mean RT and ER.

This paper is organized as follows. First, we formalize the model developed in [17] and introduce the SERIA model. Second, we describe our experimental setup. Third, we present our behavioral findings in terms of summary statistics (mean RT and ER), the comparison between different models, and the parameter estimates. Finally, we review our findings, discuss other recent models, potential future developments, and translational applications.

Materials and methods

Ethics statement

All participants gave written informed consent before the study. All experimental procedures were approved by the local ethics board (Kantonale Ethikkommission Zürich, KEK-ZH-Nr.2014-0246).

Race models for antisaccades

In this section, we derive a formal description of the models evaluated in this paper. We start with a formalized version of the model proposed by Noorani and Carpenter in [17] and proceed to extend it. Their approach resembles the model originally proposed by Camalier and colleagues [21] to explain RT and ER in the double step and search step tasks, in which participants are either asked to saccade to successively presented targets or to saccade to a target after a distractor was shown. Common to all these tasks is that subjects are required to inhibit a prepotent reaction to an initial stimulus and then to generate an action towards a secondary goal. Briefly, Camalier and colleagues [21] extended the original ‘horse-race’ model [16] by including a secondary action in countermanding tasks. In [17], Noorani and Carpenter used a similar model in combination with the LATER model [22] in the context of the antisaccade task by postulating an endogenously generated inhibitory signal. Note that this model, or variants of it, have been used in several experimental paradigms (reviewed in [20]). Here, we limit our discussion to the antisaccade task.

The pro, stop, and antisaccade model (PROSA)

Following [17], we assume that the RT and the type of saccade generated in a given trial are caused by the interaction of three competing processes or units. The first unit u_p represents a command to perform a prosaccade, the second unit u_s represents an inhibitory command to stop a prosaccade, and the third unit u_a represents a command to perform an antisaccade. The time t required for unit u_i to arrive at threshold s_i is given by:

$$s_i = r_i t, \tag{1}$$

$$\frac{s_i}{r_i} = t, \tag{2}$$

where r_i represents the slope or increase rate of unit u_i , s_i represents the height of the threshold, and t represents time. We assume that, on each trial, the increase rates are stochastic and independent of each other.

The time and order in which the units reach their thresholds s_i determines the action and RT in a trial. If the prosaccade unit u_p reaches threshold before any other unit at time t , a prosaccade is elicited at t . If the antisaccade unit arrives first, an antisaccade is elicited at t . Finally, if the stop unit arrives before the prosaccade unit, an antisaccade is elicited at the time when the antisaccade unit reaches threshold. It is worth mentioning that, although this model is motivated as a race-to-threshold model, actions and RTs depend only on the arrival times of each of the units and ultimately no explicit model of increase rates or thresholds is required. Thus, for the sake of clarity, we refer to this approach as a ‘race’ model, in contrast to ‘race-to-threshold’ models that explicitly describe increase rates and thresholds.

Formally (but in a slight abuse of language), the two random variables of interest, the reaction time $T \in [0, \infty[$ and the type of action performed $A \in \{pro, anti\}$, depend only on three further random variables: the arrival times $U_p, U_s, U_a \in [0, \infty[$ of each of the units. The

probability of performing a prosaccade at time t is given by the probability of the prosaccade unit arriving at time t , and the stop and antisaccade unit arriving afterwards:

$$p(A = pro, T = t) = p(U_p = t)p(U_a > t)p(U_s > t). \tag{3}$$

The probability of performing an antisaccade at time t is given by

$$p(A = anti, T = t) = p(U_a = t)p(U_p > t)p(U_s > t) + p(U_a = t) \int_0^t p(U_s = \tau)p(U_p > \tau)d\tau. \tag{4}$$

The first term on the right side of Eq 4 corresponds to the unlikely case that the antisaccade unit arrives before the prosaccade and the stop units. The second term describes trials in which the stop unit arrives before the prosaccade unit. It can be decomposed into two terms:

$$p(U_a = t) \int_0^t p(U_s = \tau)p(U_p > \tau)d\tau = p(U_a = t) \left(p(U_s < t)p(U_p > t) + \int_0^t p(U_s = \tau)p(\tau < U_p < t)d\tau \right) \tag{5}$$

$$= p(U_a = t) \left(p(U_s < t)p(U_p > t) + \int_0^t p(U_s < \tau)p(U_p = \tau)d\tau \right) \tag{6}$$

The term $p(U_a = t) \int_0^t p(U_s < \tau)p(U_p = \tau)d\tau$ describes the condition in which the prosaccade unit is inhibited by the stop unit allowing for an antisaccade. Note that if the prosaccade unit arrives later than the antisaccade unit, the arrival time of the stop unit is irrelevant. That means that we can simplify Eq 4 to

$$p(A = anti, T = t) = p(U_a = t) \left(p(U_p > t) + \int_0^t p(U_s < \tau)p(U_p = \tau)d\tau \right). \tag{7}$$

Eqs 3 and 7 constitute the likelihood function of a single trial, and define the joint probability of an action and the corresponding RT. We refer to this likelihood function as the PRO-Stop-Antisaccade (PROSA) model. It shares the central assumptions of [17], namely: (i) the time to reach threshold of each of the units is assumed to depend linearly on the rate r , (ii) it includes a stop unit whose function is to inhibit prosaccades and (iii) there is no lateral inhibition between the different units. Finally, (iv) RTs are assumed to be equal to the arrive-at-threshold times. Note that the RT distributions are different from the arrival time distributions because of the interactions between the units described above. The main difference of this model compared to [17] is that we do not exclude *a priori* the possibility of the antisaccade unit arriving earlier than the other units. Aside from this, both models are conceptually equivalent.

The Stochastic Early Reaction, Inhibition, and Late Action Model (SERIA)

The PROSA model is characterized by a strict association between units and action types. In other words, the unit u_p leads unequivocally to a prosaccade, whereas the unit u_a always triggers an antisaccade. This implies that if the distribution of the arrival times of the units is unimodal and strictly positive, the PROSA model cannot predict voluntary slow prosaccades with a late peak, or in simple words, the PROSA model cannot account for slow, voluntary prosaccades that have been postulated in the antisaccade task [23]. Similarly, it has been argued that prosaccade RT can be described by the mixture of two distributions (for example [2,22]). To account for this, we introduce the Stochastic Early Reaction, Inhibition and Late Action (SERIA) model.

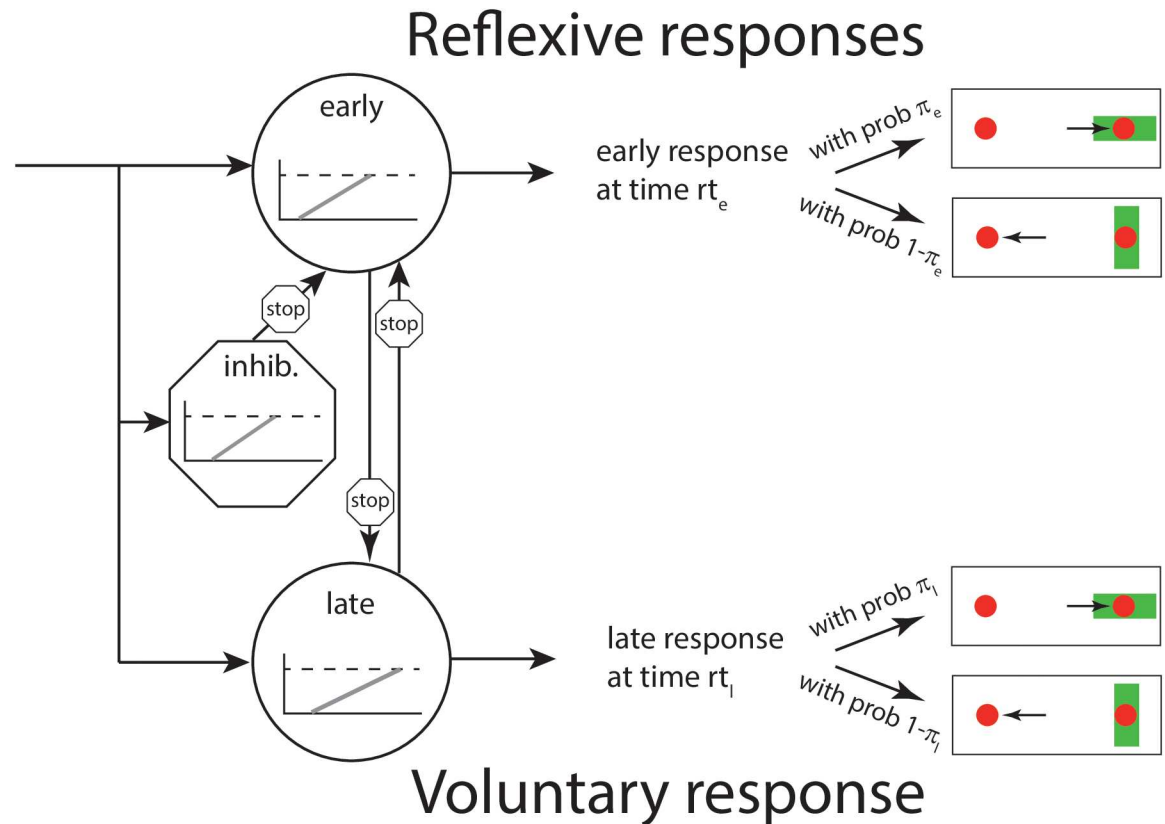


Fig 1. Layout of the SERIA model. The presentation of a visual cue (a green bar) triggers the race of three independent units. The inhibitory unit can stop an early response. Importantly, both early and late responses can trigger pro- and antisaccades. Note that the PROSA model is a special case of the SERIA model in which $\pi_e = 1$ and $\pi_l = 0$, i.e. all early responses are prosaccades, whereas all late responses are antisaccades.

<https://doi.org/10.1371/journal.pcbi.1005692.g001>

According to this model, and in analogy to the PROSA model, an early reaction takes place at time t if the early unit u_e arrives before the late and inhibitory units, u_l and u_i , respectively. If the inhibitory or late unit arrives before the early unit, a late response is triggered at the time the late unit reaches threshold. Crucially, both early and late responses can trigger pro- and antisaccades with a certain probability. Thus, in parallel to the race processes which determine RTs, an independent, secondary decision process is responsible for which reaction is generated. Fig 1 shows the structure of the SERIA model.

To formalize the concept of early and late responses, we introduce a new unobservable random variable that represents the type of response $R \in \{early, late\}$. The distribution of the RTs is analogous to the PROSA-model, such that, for instance, the probability of an early response at time t is given by

$$p(R = early, T = t) = p(U_e = t)p(U_i > t)p(U_l > t) \tag{8}$$

where U_e , U_i , and U_l represent the arrival times of the early, inhibitory, and late units, respectively. The fundamental assumption of the SERIA model is that a secondary decision process, beyond the race between early, inhibitory, and late units, decides the action generated in a single trial. An initial approach to model this secondary decision process is to assume that the action type (pro- or antisaccade) is conditionally independent of the RT given the response

type (early or late). Hence, the distribution of RTs is not *a priori* coupled to the saccade type anymore; RT distributions for both pro- and antisaccades could in principle be bimodal, consisting of both fast reactive and slow voluntary saccades.

Formally, the conditional independency assumption can be written down as

$$p(A, T|R) = p(A|R)p(T|R), \tag{9}$$

$$p(A, T|R)p(R) = p(A|R)p(T|R)p(R), \tag{10}$$

$$p(A, T, R) = p(A|R)p(T, R). \tag{11}$$

The term $p(A|R)$ is simply the probability of an action, given a response type. We denote it as

$$p(A = \textit{pro}|R = \textit{early}) = \pi_e \in [0, 1], \tag{12}$$

$$p(A = \textit{anti}|R = \textit{early}) = 1 - \pi_e, \tag{13}$$

$$p(A = \textit{pro}|R = \textit{late}) = \pi_l \in [0, 1], \tag{14}$$

$$p(A = \textit{anti}|R = \textit{late}) = 1 - \pi_l. \tag{15}$$

Since the type of response R is not observable, it is necessary to marginalize it out in Eq 11 to obtain the likelihood of the SERIA model:

$$p(A, T) = p(A, T, R = \textit{early}) + p(A, T, R = \textit{late}). \tag{16}$$

The complete likelihood of the model is given by substituting the terms in Eq 16

$$p(A = \textit{pro}, T = t) = \pi_e p(U_e = t) p(U_i > t) p(U_l > t) + \pi_l p(U_l = t) \left(p(U_e > t) + \int_0^t p(U_e = \tau) p(U_i < \tau) d\tau \right), \tag{17}$$

$$p(A = \textit{anti}, T = t) = (1 - \pi_e) p(U_e = t) p(U_i > t) p(U_l > t) + (1 - \pi_l) p(U_l = t) \left(p(U_e > t) + \int_0^t p(U_e = \tau) p(U_i < \tau) d\tau \right). \tag{18}$$

It is worth noting here that the PROSA model is a special case of the SERIA model, namely, it corresponds to the assumption that $\pi_e = 1$ and $\pi_l = 0$. The SERIA model allows for bimodal distributions, as both early and late responses can be pro- and antisaccades. Importantly, one prediction of the model is that late prosaccades have the same distribution as late antisaccades.

A late race competition model for saccade type

Until now, we have assumed that the competition that leads to late pro- and antisaccades does not depend on time in the sense that late actions are conditionally independent of RT. This assumption can be weakened by postulating a secondary race between late responses; this leads us to a modified version of the SERIA model, that we refer to as the late race SERIA model (SERIA_{lr}). The derivation proceeds similarly to the SERIA model, except that we postulate a fourth unit that generates late prosaccades instead of assuming that the late decision process is time insensitive.

This version of the SERIA model includes an early unit u_e that, for simplicity, we assume produces only prosaccades, an inhibitory unit that stops early responses u_i , a late unit that triggers antisaccades u_a , and a further unit that triggers late prosaccades u_p . As before, if the early unit reaches threshold before any other unit, a prosaccade is generated with probability

$$p(U_e = t)p(U_i > t)p(U_a > t)p(U_p > t). \tag{19}$$

If any of the late units arrive first, the respective action is generated with probability:

$$\text{Antisaccade : } p(U_a = t)p(U_p > t)p(U_e > t)p(U_i > t). \tag{20}$$

$$\text{Prosaccade : } p(U_p = t)p(U_a > t)p(U_e > t)p(U_i > t). \tag{21}$$

Finally, if the inhibitory unit arrives first, either a late pro- or antisaccade is generated with probability

$$\text{Antisaccades : } p(U_a = t)p(U_p > t) \left(\int_0^t p(U_i = \tau)p(U_e > \tau)d\tau \right), \tag{22}$$

$$\text{Prosaccades : } p(U_p = t)p(U_a > t) \left(\int_0^t p(U_i = \tau)p(U_e > \tau)d\tau \right). \tag{23}$$

Implicit in the last two terms is the competition between the late units, which are assumed again to be independent of each other. Formally, this competition is expressed as the probability of, for example, the late antisaccade unit arriving before a late prosaccade $p(U_a = t)p(U_p > t)$. A schematic representation of the model is shown in Fig 2. This late race is similar to the Linear Ballistic Accumulation model proposed by [24], although in that model decisions are seen as the result of a race of ballistic accumulation processes with fixed threshold but stochastic base line and increase rate. Here we only assume that the late decision process is a GO-GO race [21].

The likelihood of an action is given by summing over all possible outcomes that lead to that action:

$$p(A = pro, T = t) = p(U_e = t)p(U_i > t)p(U_a > t)p(U_p > t) + p(U_p = t)p(U_a > t)p(U_i > t)p(U_e > t) + p(U_p = t)p(U_a > t) \left(\int_0^t p(U_i = \tau)p(U_e > \tau)d\tau \right), \tag{24}$$

$$p(A = anti, T = t) = p(U_a = t)p(U_p > t)p(U_i > t)p(U_e > t) +$$

$$p(U_a = t)p(U_p > t) \left(\int_0^t p(U_i = \tau)p(U_e > \tau)d\tau \right). \tag{25}$$

We have left out some possible simplifications in Eqs 24 and 25 for the sake of clarity.

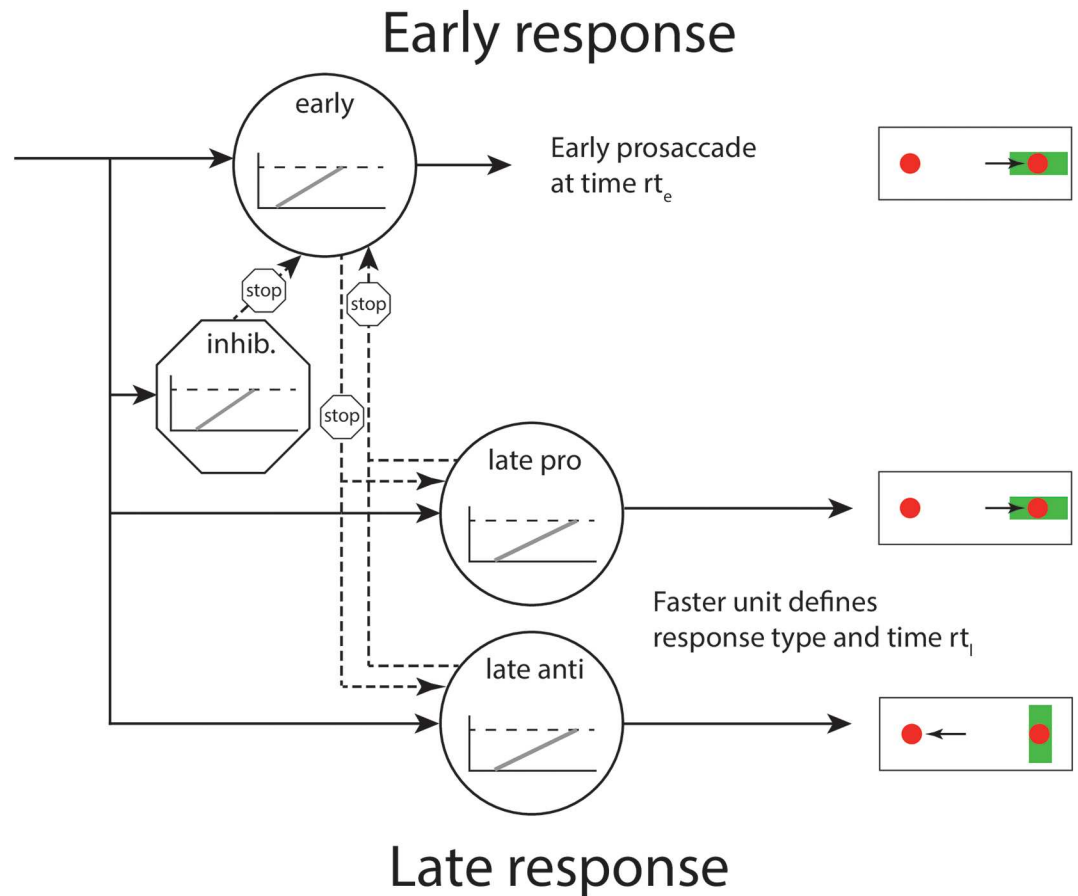


Fig 2. Layout of the SERIA_r model. The presentation of a visual cue (a green bar) triggers the race of four independent units. The inhibitory unit can stop an early response. The late decision process is triggered by the competition between two further units.

<https://doi.org/10.1371/journal.pcbi.1005692.g002>

The conditional probability of a late antisaccade is given by the interaction between the late units, such that

$$p(U_a < U_p) = \int_0^{\infty} p(U_a = t)p(U_p > t)dt = 1 - p(U_p < U_a), \quad (26)$$

is analogous to the probability of a late antisaccade $1 - \pi_l$ in the SERIA model. This observation shows that the main difference between the SERIA and SERIA_r model is that the former postulates that the distribution of late pro- and antisaccades are equal and conditionally independent of the action performed, whereas the latter constrains the probability of a late antisaccade to be a function of the arrival times of the late units.

The expected *response time* of late pro- and antisaccade actions is given by

$$\frac{1}{p(U_p < U_a)} \int_0^{\infty} t p(U_p = t)p(U_a > t)dt, \quad (27)$$

$$\frac{1}{p(U_a < U_p)} \int_0^\infty t p(U_a = t) p(U_p > t) dt. \tag{28}$$

We will refer to these terms as the mean *response time* of pro- and antisaccade actions, in contrast to the mean arrival times, which are the expected value of any single unit.

Non-decision time

The models above can be further finessed to account for non-decision times δ by transforming the RT t to $t_\delta = t - \delta$. The delay δ might be caused by, for example, conductance delays from the retina to the cortex. In addition, the antisaccade or late units might include a constant delay δ_a , which is often referred to as the antisaccade cost [1]. Note that the model is highly sensitive to δ because any RT below it has zero probability. In order to relax this condition and to account for early outliers, we assumed that saccades could be generated before δ at a rate $\eta \in [0,1]$ such that the marginal likelihood of an outlier is

$$p(T < \delta) = p(T_\delta < 0) = \eta. \tag{29}$$

For simplicity, we assume that outliers are generated with uniform probability in the interval $[0, \delta]$:

$$p(T = t) = \frac{\eta}{\delta} \text{ if } t < \delta. \tag{30}$$

Furthermore, we assume that the probability of an early outlier being a prosaccade was approximately 100 times higher than being an antisaccade. Because of the new parameter η , the distribution of saccades with a RT larger than δ needs to be renormalized by the factor $1 - \eta$. In the case of the PROSA model, for example, this means that the joint distribution of action and RT is given by the conditional probability

$$p(A = \textit{pro}, T = t_\delta | t_\delta > 0) = p(U_p = t_\delta) p(U_a > t_\delta - \delta_a) p(U_s > t_\delta), \tag{31}$$

$$p(U_a < 0) = 0, \tag{32}$$

$$p(A = \textit{anti}, T = t_\delta | t_\delta > 0) = p(U_a = t_\delta - \delta_a) \left(p(U_p > t_\delta) + \int_0^{t_\delta} p(U_p = \tau) p(U_s < \tau) d\tau \right). \tag{33}$$

A similar expression holds for the SERIA models. However, in the PROSA model a unit-specific delay is equal to an action-specific delay. By contrast, in the SERIA model both early and late responses can generate pro- and antisaccades. Thus, δ_a represents a delay in the late actions that affects both late pro- and antisaccades.

Parametric distributions of the increase rate

The models discussed in the previous sections can be defined independently of the distribution of the rate of each of the units. In order to fit experimental data, we considered four parametric distributions with positive support for the rates: gamma [13], inverse gamma, lognormal [25] and the truncated normal distribution (similarly to [22] and [24]). Table 1 and Fig 3 summarize these distributions, their parameters, and the corresponding arrival time densities. We considered five different configurations: 1) all units were assigned *inverse gamma* distributed rates, 2) all units were assigned *gamma* distributed rates, 3) the increase rate of the prosaccade

Table 1. Parametric density functions of the increase rates.

Name	Parameters	Rate p.d.f.	Arrival time p.d.f.
Gamma	k, θ	$\frac{\theta^k}{\Gamma(k)} e^{-\theta/r} r^{k-1}$	$\frac{\theta^k}{\Gamma(k)} e^{-\theta/t} t^{k-1}$
Inv. gamma	k, θ	$\frac{\theta^k}{\Gamma(k)} e^{-\theta/r} r^{-k-1}$	$\frac{\theta^k}{\Gamma(k)} e^{-\theta/t} t^{k-1}$
Log normal	μ, σ^2	$\frac{1}{\sqrt{2\pi\sigma}} e^{-\frac{1}{2}(\frac{\ln r - \mu}{\sigma})^2}$	$\frac{1}{\sqrt{2\pi\sigma}} e^{-\frac{1}{2}(\frac{\ln t - \mu}{\sigma})^2}$
T. normal	μ, σ^2	$\frac{1}{Z} e^{-\frac{1}{2}(\frac{r-\mu}{\sigma})^2}$	$\frac{1}{Z} e^{-\frac{1}{2}(\frac{t-\mu}{\sigma})^2}$

Z is the normalization constant $Z = \int_0^\infty \exp\left(-\frac{(r-\mu)^2}{2\sigma^2}\right) dr$.

<https://doi.org/10.1371/journal.pcbi.1005692.t001>

and stop units (or early and the inhibitory units) was *gamma distributed* but the antisaccade (late) unit's increase rate was *inverse gamma* distributed, 4) all the units were assigned *lognormal* distributed rates or 5) all units were assigned *truncated normal* distributed rates.

All the parametric distributions considered here can be fully characterized by two parameters which we generically refer to as k and θ . Hence, the PROSA model is characterized by the parameters for each unit $k_p, k_a, k_s, \theta_p, \theta_a, \theta_s$. The SERIA model can be characterized by analogous parameters $k_e, k_p, k_i, \theta_e, \theta_p, \theta_i$ and the probabilities of early and late prosaccades π_e and π_l . In the case of the SERIA_{lr} model, the probability of a late prosaccade is replaced by the parameters of a late prosaccade unit k_p, θ_p . In addition to the unit parameters, all models included the non-decision time δ , the antisaccade (or late unit) cost δ_a , and the marginal rate of early outliers η .

Experimental procedures

In this section, we describe the experimental procedures, statistical methods, and inference scheme used to invert the models above. The data is from the placebo condition of a larger pharmacological study that will be reported elsewhere.

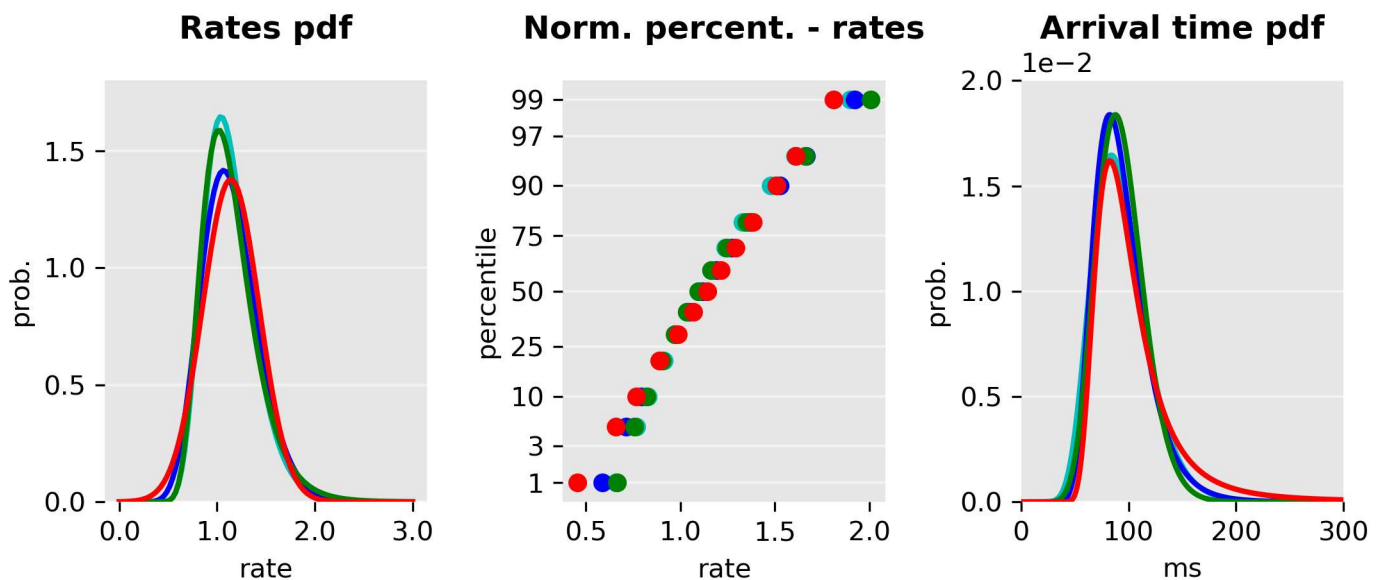


Fig 3. Illustration of probability distributions used to model increase rates. Left: Distribution of the rates based on different probability density functions: Normal (red), gamma (blue), inverse gamma (green), and log-normal (cyan). All distributions were matched to have equal mean and variance. Center: Probit plots of the same distributions. While the gamma and lognormal distributions are very close to the straight line induced by the normal distribution, the inverse gamma distribution diverges slightly more from linearity. Right: Arrival time distribution (scaled to ms).

<https://doi.org/10.1371/journal.pcbi.1005692.g003>

Participants. Fifty-two healthy adult males naïve to the antisaccade task were invited to a screening session through the recruitment system of the Laboratory of Social and Neural Systems Research of the University of Zurich. During screening, and after being debriefed about the experiment, subjects underwent an electrocardiogram, a health survey, a visual acuity test, and a color blindness test. Subjects were excluded if any of the following criteria were met: age below 18 or above 40 years, regular smoking, alcohol consumption the day before the experiment, any possible interaction between current medication and levodopa or benserazide, pulse outside the range 55–100bpm, recreational drug intake in the past 6 months, history of serious mental or neurological illness, or if the medical doctor supervising the experiment deemed the participant not apt. All subjects gave their written informed consent to participate in the study and received monetary compensation.

Procedure. Each subject was invited to two sessions. During both visits, the same experimental protocol was followed. After arrival, placebo or levodopa (Madopar DR 250, 200mg of levopa + 50 mg benserazide) was orally administered in the form of shape- and color-matched capsules. The present study is restricted to data from the session in which subjects received placebo. Participants and experimenters were not informed about the identity of the substance. Immediately afterwards subjects were introduced to the experimental setup and to the task through a written document. This was followed by a short training block (see below).

The experiment started 70 minutes after substance administration. Subjects participated in three blocks of 192 randomly interleaved pro- and antisaccade trials. The percentages of prosaccade trials in the three blocks were 20%, 50%, or 80%. This yielded three *prosaccade probability* (PP) conditions: PP20, PP50, and PP80. Thus, in the PP20 block, subjects were presented a prosaccade cue in 38 trials, while in all other 154 trials an antisaccade cue was shown. The order of the trials was randomized in each block, but the same order was used in all subjects and sessions. The order of the conditions was counterbalanced across subjects.

Stimulus and apparatus. During the experiment, subjects sat in front of a CRT monitor (Philipps 20B40, distance eye-screen: $\approx 60\text{cm}$, refresh rate: 75Hz). The screen subtended a horizontal visual angle of 38 degrees of visual angle (dva). Eye movements were recorded using a remote infrared camera (Eyelink II, SR-Research, Canada). Participants' head was stabilized with a chin rest. Data were stored at a sampling rate of 500 Hz.

During the task, two red dots (0.25dva) that constituted the saccadic targets were constantly displayed at an eccentricity of $\pm 12\text{dva}$. Displaying the saccadic target before the execution of an antisaccade has been reported to affect saccadic velocity and accuracy, but not RTs [26], and arguably decreases the need for sensorimotor transformations [27]. At the beginning of each trial, a gray fixation cross ($0.6 \times 0.6\text{ dva}$) was displayed at the center of the screen. After a random fixation interval (500 to 1000 ms), the cross disappeared, and the cue instructing either a pro- or an antisaccade trial (see below) was shown centered on either of the red dots. As mentioned above, in each block, subjects were presented with a prosaccade cue in either 20, 50, or 80 percent of the trials. The order of the presentation of the cues was randomized. The cue was a green rectangle ($3.48 \times 0.8\text{ dva}$) displayed for 500ms in either horizontal (prosaccade) or vertical orientation (antisaccade). Once the cue was removed and after 1000ms, the next trial started.

Subjects were instructed to saccade in the direction of the cue when a horizontal bar was presented (prosaccade trial) and to saccade in the opposite direction when a vertical bar was displayed (antisaccade trial, see Fig 4). See [28,29] for similar task designs.

Prior to the main experiment, participants were trained on the task in a block of 50 prosaccade trials, immediately followed by 50 antisaccade trials. During the training, subjects were automatically informed after each trial whether their response was correct or not (see below), or whether they had failed to produce a saccade within 500ms after cue presentation (CP). No feedback was given during the main experimental blocks.

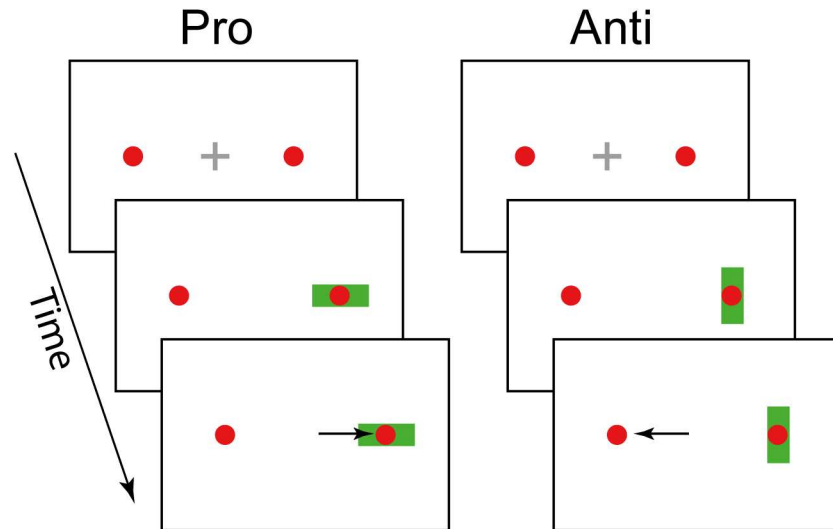


Fig 4. Task design. After a variable fixation period of 500–1000ms (top) the cue (green rectangle) appeared on the screen for 500 ms. The orientation of the cue (horizontal or vertical) indicated the required response (prosaccade or antisaccade).

<https://doi.org/10.1371/journal.pcbi.1005692.g004>

Data preparation. Data were parsed and preprocessed using the Python programming language (2.7). Saccades were detected using the algorithm provided by the eyetracker manufacturer (SR Research), which uses a velocity and acceleration threshold of $22dva/s$ and $3800dva/s^2$ [30]. We only considered saccades with a magnitude larger than $2dva$. RT was defined as the time between CP and the first saccade larger than $2dva$. A prosaccade trial was considered correct if the end position of the saccade was ipsilateral to the cue and, conversely, an antisaccade trial was considered correct if the end position of the saccade was contralateral to the cue.

Trials were excluded from further analysis if a) data were missing, b) a blink occurred between CP and the main saccade, c) the trial was aborted by the experimenter, d) subjects failed to fixate in the interval between fixation detection and CP, e) if a saccade was detected only later than 800ms after CP, f) if the RT was below 50ms, and in the case of an antisaccade if it was below 110ms. Corrective antisaccades were defined as saccades that a) followed a prosaccade error, b) occurred no later than 900ms after CP, and c) had less than $3dva$ horizontal error from the red circle contralateral to the cue.

Besides the fitted non-decision time δ we assumed a fixed non-decision time of 50ms for all participants [17]. This was implemented by subtracting 50ms of all saccades before being entered into the model. In order to avoid numerical instabilities, RT were rescaled from millisecond to tenths of a second during all numerical analysis. All results are presented in ms.

Modeling

We aimed to answer three questions with the models considered here. First, we investigated which model (i.e. PROSA, SERIA or SERIA_{lr}) explained the experimental data best, and whether all important qualitative features of the data were captured by this model. We did not have a strong hypothesis regarding the parametric distribution of the data and hence, comparisons of parametric distributions were only of secondary interest in our analysis. Second, we investigated whether reduced models that kept certain parameters fixed across trial types were

Table 2. Model families with the respective increase-rate distributions.

Model	PROSA		
	Prosaccade/ stop units	Anti. unit	# Param. full/const.
m_1/m_1^c	Inv. gamma	Inv. gamma	15/13
m_2/m_2^c	Gamma	Gamma	15/13
m_3/m_3^c	Gamma	Inv. gamma	15/13
m_4/m_4^c	Lognorm.	Lognorm.	15/13
m_5/m_5^c	T. norm.	T. norm.	15/13
SERIA			
	Early/stop units	Late unit	
m_6/m_6^c	Inv. gamma	Inv. gamma	19/13
m_7/m_7^c	Gamma	Gamma	19/13
m_8/m_8^c	Gamma	Inv. gamma	19/13
m_9/m_9^c	Lognorm.	Lognorm.	19/13
m_{10}/m_{10}^c	T. norm.	T. norm.	19/13
SERIA _{lr}			
	Early/stop units	Late pro./anti. units	
m_{11}/m_{11}^c	Inv. gamma	Inv. gamma	19/15
m_{12}/m_{12}^c	Gamma	Gamma	19/15
m_{13}/m_{13}^c	Gamma	Inv. gamma	19/15
m_{14}/m_{14}^c	Lognorm.	Lognorm.	19/15
m_{15}/m_{15}^c	T. norm.	T. norm.	19/15

Models with parameters constrained to be equal across trial types are referred through the superscript *c*.

<https://doi.org/10.1371/journal.pcbi.1005692.t002>

sufficient to model the data. Third, we investigated how the probability of a trial type in a block affected the parameters of the model.

Model space. Initially, we considered 15 different models as shown in Table 2. Each model was fitted independently for each subject and condition. Since our experimental design included mixed blocks, we allowed for different parameters in pro- and antisaccade trials, i.e., different increase-rate distributions depending on the *trial type* (TT). Under this hypothesis, the PROSA model had 12 free parameters (6 for each TT), whereas the SERIA model required 4 further parameters (π_e and π_l in each TT). The late race SERIA_{lr} model included 16 parameters for the units (8 for each TT). We did not investigate the case that early reactions could trigger antisaccades but rather fixed the probability of an early antisaccade $1 - \pi_e$ to 10^{-3} . The rationale behind this was that if early reactions are a priori assumed to never trigger antisaccades, rare but possible early antisaccades might cause large biases when fitting a model.

Regarding the non-decision time δ , antisaccade cost δ_a , and rate of outliers η , we assumed equal parameters in both TT. Consequently, the full PROSA model had 15 free parameters whereas the full SERIA and SERIA_{lr} models had both 19 free parameters.

In addition to the full models, we evaluated restricted versions of each of them by constraining some parameters to be equal across TT. In the case of the SERIA model, we hypothesized that the parameters of all units were equal, irrespective of TT (i.e., that the rate of the units was not affected by the cue presented in a trial). However, we assumed that the probability that an early or late response was a prosaccade was different in pro- and antisaccade trials. Therefore, in the case of the SERIA model, instead of 12 unit parameters (6 per TT), the restricted model had only 6 parameters for the units' rates. The parameters π_e and π_l were allowed to differ in

pro- and antisaccade trials. In the case of the restricted SERIA_{lr} model, the units that underlie the late decision process were allowed to vary across TT, yielding a restricted model with 4 parameters for the early and inhibitory units, and 8 for the late decision process, half of them for each trial type. In the case of the PROSA model, similarly to [17], it is possible to assume that the parameters of the prosaccade unit remain constant across TT, and that the parameters of the stop and antisaccade units depend on TT, yielding 10 parameters for the units.

Prior distributions for model parameters. To complete the definition of the models, the prior distribution of the parameters was specified. This distribution reflects beliefs that are independent of the data and provides a form of regularization when inverting a model. In order to avoid any undesired bias regarding the parametric distributions considered here, we reparametrized all but the truncated normal distribution in terms of their mean and variance. We then assumed that the log of the mean and variance of the rate of the units were equally normally distributed (see Table 3). Therefore, the parametric distributions had the same prior in terms of their first two central moments. In the case of the truncated normal distribution, instead of an analytical transformation between its first two moments and its natural parameters μ and σ^2 , we defined the prior distribution as a density of μ and $\ln \sigma^2$. To ensure that μ was positive with high probability (96%) we assumed that $\mu \sim N(0.55, 0.09)$. The variance term was distributed as displayed in Table 3. As a further constraint, we restricted the parameter space to enforce that the first two moments of the distributions of rates and RTs existed. We relaxed this constraint for the late units of the SERIA_{lr} in order to allow for ‘flat’ distributions with possibly infinite mean and variance. This can describe a case in which the increase rate of one of the late units is extremely low.

For the non-decision time δ and the antisaccade cost δ_a , the prior of their log transform was a normal distribution, consistent across all models. Note that the scale of the parameters δ and δ_a in Table 3 is tenths of a second. The fraction of early outliers η , and early and late prosaccades π_e and π_l were assumed to be Beta distributed, with parameters 0.5 and 0.5. Thus, for example, the prior probability of an early outlier is given by

$$p(\eta) \propto \eta^{0.5}(1 - \eta)^{0.5}. \tag{34}$$

This parametrization constitutes the minimally informative prior distribution, as it is the Jeffrey’s prior of η , π_e and π_l . Table 3 displays the parameters used for the prior distributions.

Bayesian inference

Inference on the model parameters was performed using the Metropolis-Hastings algorithm [31]. To increase the efficiency of our sampling scheme, we iteratively modified the proposal distribution during an initial ‘burn-in’ phase as proposed by [32]. Moreover, we extended this method by drawing from a set of chains at different temperatures and swapping samples across chains. This method, called population MCMC or parallel tempering, increases the statistical

Table 3. Prior probability density functions.

Parameter	Probability density function	Expected value	Variance
μ_r	$\mathcal{N}(\ln \mu_r; -1.08, 0.97)$	0.55	0.5
σ_r^2	$\mathcal{N}(\ln \sigma_r^2; -2.64, 0.69)$	0.1	0.01
δ	$\mathcal{N}(\ln \delta; -1.58, 1.79)$	0.5	1.25
δ_a	$\mathcal{N}(\ln \delta_a; -0.87, 1.17)$	0.75	1.25
π_e	$Beta(\pi_e; 0.5, 0.5)$	0.5	0.145
π_l	$Beta(\pi_l; 0.5, 0.5)$	0.5	0.145
η	$Beta(\eta; 0.5, 0.5)$	0.5	0.145

<https://doi.org/10.1371/journal.pcbi.1005692.t003>

efficiency of the Metropolis-Hasting algorithm [33] and has been used in similar contexts before [34]. We simulated 16 chains with a 5-th order temperature schedule [35]. For all but the models including a truncated normal distribution, we drew 4.1×10^4 samples per chain, from which the first 1.6×10^4 samples were discarded as part of the burn-in phase. When a truncated normal distribution was included (models m_5 , m_{10} , and m_{15}), the total number of samples was increased to 6×10^4 , from which 2×10^4 were discarded. The convergence of the algorithm was assessed using the Gelman-Rubin criterion [33,36] such that the \tilde{R} statistic of the parameters of the model was aimed to be below 1.1. When a simulation did not satisfy this criterion, it was repeated until 99.5 percent of all simulations satisfied it.

Models were scored using their log marginal likelihood or log model evidence (LME). This is defined as the log probability of the data given a model after marginalizing out all its parameters. When comparing different models, the LME corresponds to the log posterior probability of a model under a uniform prior on model identity. Thus, for a single subject with data y , the posterior probability of model k , given models 1 to n is

$$p(m_k|y) = \frac{p(y|m_k)p(m_k)}{\sum_{i=1}^n p(y|m_i)p(m_i)} = \frac{p(y|m_k)}{\sum_{i=1}^n p(y|m_i)}. \quad (35)$$

Importantly, this method takes into account not only the accuracy of the model but also its complexity, such that overparameterized models are penalized [37]. A widely used approximation to the LME is the Bayesian Information Criterion (BIC) which, although easy to compute, has limitations (for discussion, see [38]). Here, we computed the LME through thermodynamic integration [33,39]. This method provides robust estimates and can be easily computed using samples obtained through population MCMC.

One important observation here is that the LME is sensitive to the prior distribution, and thus can be strongly influenced by it [40]. We addressed this issue in two ways: On one hand and as mentioned above, we defined the prior distribution of the increase rates of all models in terms of the same mean and variance. This implies that the priors were equal up to their first two moments, and hence all models were similarly calibrated. On the other hand, we complemented our quantitative analysis with qualitative posterior checks [33] as shown in the results section.

Besides comparing the evidence of each model, we also performed a hierarchical or random effects analysis described in [38,41]. This method can be understood as a form of soft clustering in which each subject is assigned to a model using the LME as assignment criterion. Here, we report the expected probability of the model r_i , which represents the percentage of subjects that is assigned to the cluster representing model i . This hierarchical approach is robust to population heterogeneity and outliers, and complements reporting the group-level LME. Finally, we compared families of models [42] based on the evidence of each model for each subject summed across conditions.

Classical statistics

In addition to a Bayesian analysis of the data, we used classical statistics to investigate the effect of our experimental manipulation on behavioral variables (mean RT and ER) and the parameters of the models. We have suggested previously [11,43,44] that generative models can be used to extract hidden features from experimental data that might not be directly captured by, for example, standard linear methods or purely data driven machine learning techniques. In this sense, classical statistical inference can be boosted by extracting interpretable data features through Bayesian techniques.

Frequentist analyses of RT, ER, and parameter estimates were performed using a mixed effects generalized linear model with independent variables *subject* (SUBJECT), *prosaccade*

probability (PP) with levels PP20, PP50 and PP80, and when pro- and antisaccade trials were analyzed together, *trial type* (TT). The factor SUBJECT was always entered as a random effect, whereas PP and TT were treated as categorical fixed effects. In the case of ER, we used the probit function as link function.

Analyses were conducted with the function *fitglme.m* in MATLAB 9.0. The significance threshold α was set to 0.05.

Implementation

All likelihood functions were implemented in the C programming language using the GSL numerical package (v.1.16). Integrals without an analytical form or well-known approximations were computed through numerical integration using the Gauss-Kronrod-Patterson algorithm [45] implemented in the function *gsl_integration_qng*. The sampling routine was implemented in MATLAB (v. 8.1) and is available as a module of the open source software package TAPAS (www.translationalneuromodeling.org/tapas).

Results

Behavior

Forty-seven subjects (age: 23.8 ± 2.9) completed all blocks and were included in further analyses. A total of 27072 trials were recorded, from which 569 trials (2%) were excluded (see Table 4).

Both ER and RT showed a strong dependence on PP (Fig 5 and Table 5). Individual data is included in the S1 Dataset and is displayed in S1 Fig. The mean RT of correct pro- and antisaccade trials was analyzed independently with two ANOVA tests with factors SUBJECT and PP. We found that in both pro- ($F_{2,138} = 46.9, p < 10^{-5}$) and antisaccade trials ($F_{2,138} = 37.3, p < 10^{-5}$) the effect of PP was significant; with higher PP, prosaccade RT decreased, whereas the RT of correct antisaccades increased. On a subject-by-subject basis, we found that between the PP20 and PP80 conditions, 91% of the participants showed increased RT in correct antisaccade trials, while 81% demonstrated the opposite effect (a decrease in RT) in correct prosaccade trials. Similarly, there was a significant effect of PP on ER in both prosaccade ($F_{2,138} = 376.1, p < 10^{-5}$) as well as in antisaccade ($F_{2,138} = 347.0, p < 10^{-5}$) trials. This effect was present in all but one participant in antisaccade trials and in all subjects in prosaccade trials. Exemplary RT data of one subject in the PP50 condition is displayed in Fig 6.

Modeling

Model comparison results. Initially, we considered the models outlined in Table 2. The LME over all participants (fixed effects analysis) and the posterior probability of all models

Table 4. Summary of trials per subject.

	Valid	Blink	Missing	Aborted	FE	Late S.	Early S.	Total
Total	26503	188	60	42	249	0	30	27072
Mean	563.9	4.0	1.3	0.9	5.3	0.0	0.6	576
Std.	9.9	5.1	2.5	1.5	5.0	0.0	1.3	-
Min.	536	0	0	0	0	0	0	-
Max.	576	22	15	6	19	0	8	-

FE: Fixation errors. Late saccades are saccades elicited after 800ms. Early saccades are prosaccades elicited before 50ms after CP or antisaccades elicited before 110ms after CP.

<https://doi.org/10.1371/journal.pcbi.1005692.t004>

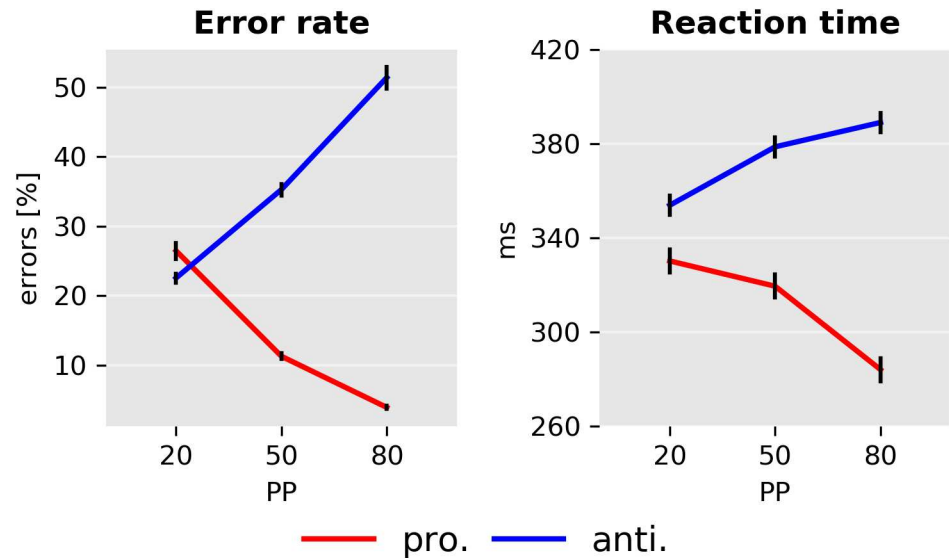


Fig 5. Error rate and mean reaction time as a function of prosaccade trial probability (PP). Left panel: Mean error rates for pro- and antisaccade trials. Right panel: Mean reaction time in ms. Error bars indicate standard errors of the mean. Only correct responses are displayed.

<https://doi.org/10.1371/journal.pcbi.1005692.g005>

and all subjects are presented in Fig 7. Independently of the particular parametric distribution of the units, the SERIA_{lr} models had higher evidence compared to the PROSA and SERIA models. A random effects, family-wise model comparison [42] resulted in an expected frequency of $r = 87\%$ for the SERIA_{lr} family, $r = 11\%$ for the SERIA family, and $r = 2\%$ for the PROSA family. In addition, constraining the parameters to be equal across trial types increased the model evidence irrespective of the parametric distribution assigned to the units (Fig 7). Here, the family-wise model comparison showed that models with constrained parameters had an expected frequency of $r = 98\%$. Over all 30 models, m_{13}^c (SERIA_{lr} with constrained parameters, early and inhibitory increase rates gamma distributed, and late units' rate inverse gamma distributed) showed the highest LME with $\Delta LME > 200$ compared to all other models. Following [40], a difference in LME larger than 3 corresponds to strong evidence.

To verify that the SERIA_{lr} family was not preferred simply because the probability of early prosaccades was fixed, we considered models in the SERIA family with the same property (not displayed). We found that although fixing this value increased the LME of the SERIA family,

Table 5. Summary of mean RTs and ERs.

Trial type	Action	Reaction times [ms]		
		PP 20	PP 50	PP80
Pro.	Pro.	330(72)	319(67)	284(59)
Pro.	Anti.	326(68)	329(46)	336(57)
Anti.	Anti	354(60)	378(57)	389(61)
Anti.	Pro	234(50)	231(47)	225(31)
		Error rates [%]		
Pro.		26(15)	11(8)	4(4)
Anti.		23(17)	35(21)	51(20)

Standard deviations are shown in brackets.

<https://doi.org/10.1371/journal.pcbi.1005692.t005>

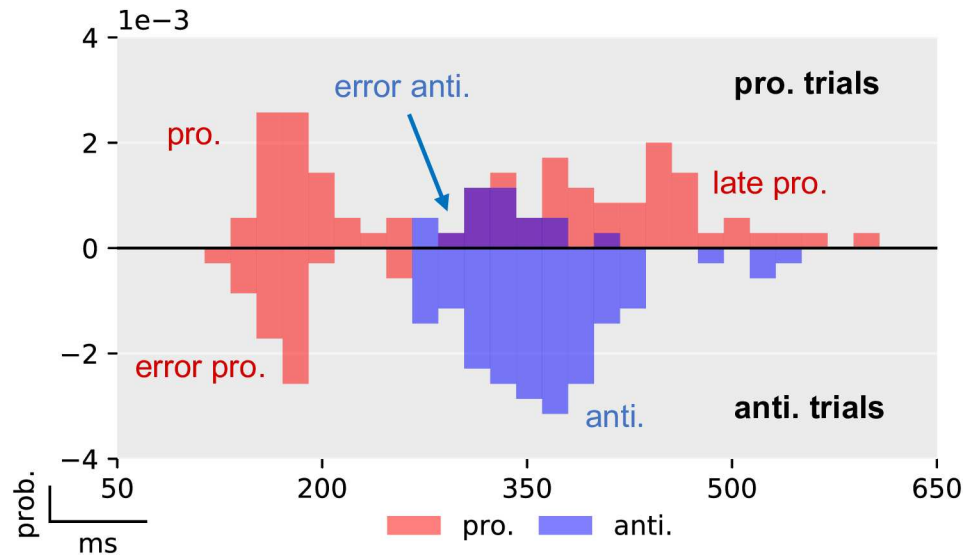


Fig 6. Exemplary histogram of the reaction times of one subject in the PP50 condition. Prosaccade trials are displayed in the upper half plane and antisaccade trials in the lower (negative) half plane. Prosaccade actions are depicted in red color, whereas antisaccade actions are shown in blue. Errors in prosaccade trials are antisaccades that for this subject occurred after the first peak of early prosaccades. Errors in antisaccade trials (lower half plane) occurred at a similar latency as early prosaccades in prosaccade trials. The histograms have been normalized to have unit probability mass, i.e., the sum of the area of all bars is one.

<https://doi.org/10.1371/journal.pcbi.1005692.g006>

there was still a difference of $\Delta LME > 90$ when comparing the best model of the $SERIA_{lr}$ family and the best model of the SERIA family with a fix probability of early prosaccades.

Fits of four subjects using the posterior samples of the best PROSA (m_1), SERIA (m_8^c), and $SERIA_{lr}$ (m_{13}^c) models are depicted in Fig 8. Although model m_1 was the best model in the PROSA family, it clearly did not explain the apparent bimodality of the prosaccade RT distributions. Instead, RTs were explained through wider distributions. No obvious difference could be observed between the SERIA and $SERIA_{lr}$ models. We further examined the model fits in Fig 9 and Fig 10 by plotting the weighted fits and cumulative density functions of the reciprocal RT in the probit scale (reciprobit plot [22]) collapsed across subjects for the best model of each family. The histograms of RTs clearly show a large number of late prosaccades whose distribution is similar to the distribution of antisaccade RTs. The most pronounced—but still small—difference between the SERIA and $SERIA_{lr}$ models was visible in prosaccade trials in the PP20 condition (left panel, upper half plane), in which antisaccade errors displayed lower RT than correct late prosaccades.

Corrective antisaccades. The RTs of antisaccades that follow an error prosaccade were not directly modeled. However, we hypothesized that corrective antisaccades are delayed late antisaccade actions, whose distribution is given by the *response time* distribution of late antisaccades

$$\frac{1}{p(U_a < U_p)} p(U_a = t) p(U_p > t) \tag{36}$$

A total of 2989 corrective antisaccades were included in the analysis. The mean (\pm std) end time of the erroneous prosaccades was 268(\pm 63)ms. The mean RT of corrective antisaccades was 447(\pm 103)ms, and the weighted mean arrival time of the late antisaccade unit was 367ms. Fig 11 displays the histogram of the end time of all prosaccade errors, the RT of all corrective

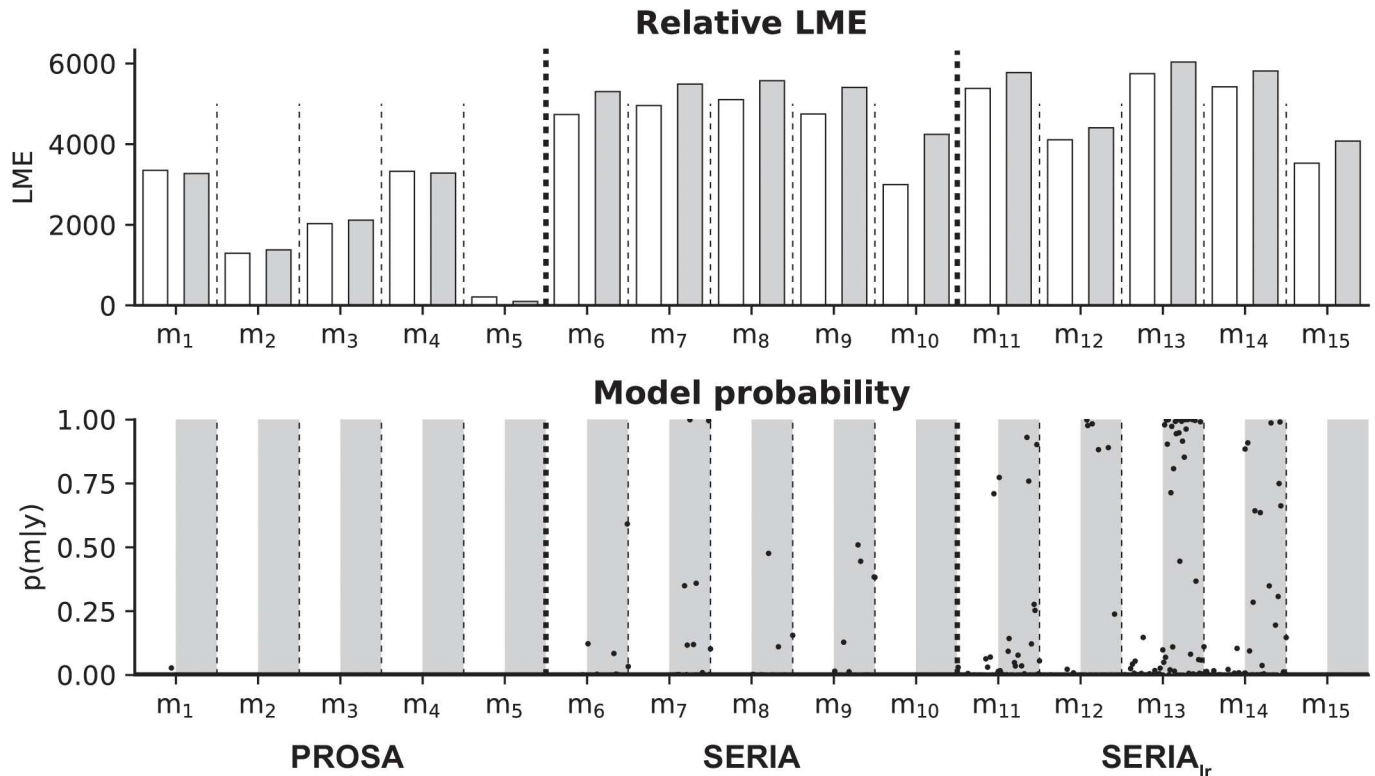


Fig 7. Summary of model comparison. Top: Summed LME of all subjects for all 30 models. White bars show models with all parameters free, grey bars models with constrained parameters. LMEs are normalized by subtracting the lowest LME (m_5). Model m_{13}^c (constrained SERIA_{Ir}) exceeded all other models ($\Delta LME > 200$). Bottom: Illustration of model probability for all subjects. The posterior model probabilities for all subjects are shown as black dots. In white shading are models with all parameters free, grey bars represent models with restricted parameters. Note that in nearly all subjects, the SERIA_{Ir} models with restricted parameters showed high model probabilities.

<https://doi.org/10.1371/journal.pcbi.1005692.g007>

antisaccades and the time shifted (+80ms) predicted response time of late antisaccades. Since we did not have a strong hypothesis regarding the magnitude of the delay of the corrective antisaccades, we selected the time shift to be the difference between the mean corrective antisaccade RT and the mean predicted response time of late antisaccades. Visual inspection strongly suggests that the distribution of corrective antisaccade RTs is well approximated by the distribution of the late responses. The short difference between corrective antisaccades' RT and the expected response time of the late antisaccade unit (80ms) favors the hypothesis that the plan for a corrective antisaccade is initiated before the incorrect prosaccade had finished.

Effects of prosaccade probability on model parameters. The effect of PP on the parameters of the model was investigated by examining the expected value of the parameters of the best scoring model (m_{13}^c). Initially, we considered the question of whether the mean arrival or response time of each of the units changed as a function of PP. For arrival times, this corresponds to

$$\frac{1}{N} \sum_{j=1}^N (E[U_i | k_j^i, \theta_j^i] + \delta_j^i) \quad (37)$$

where i is an index over the units, j is an index over N samples collected using MCMC, and δ_j^i is the estimated delay. In the case of the late units, we considered only the response time of correct actions. Fig 12 left displays the mean arrival and response times. These were submitted to

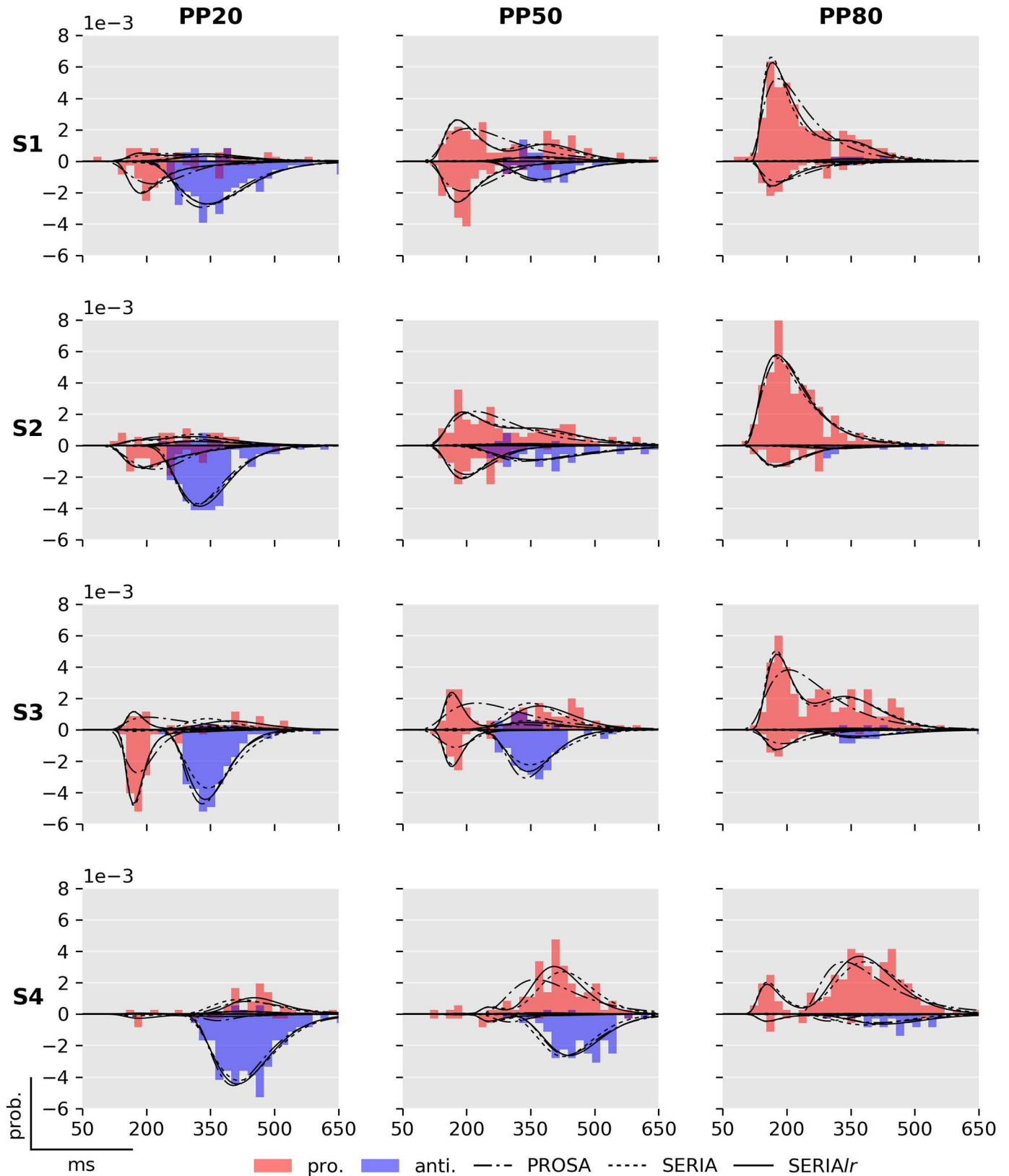


Fig 8. Fits of best PROSA (m_1), SERIA (m_6^c) and SERIA_r (m_{13}^c) models. Columns display the normalized histogram of the RTs of pro- (red) and anti- (blue) saccades in each of the conditions. Rows correspond to individual subjects named S1 to S4 for display purpose. As in Fig 6, prosaccade

trials are displayed on the upper half plane, whereas antisaccade trials are displayed in the lower half plane. The predicted RT distributions based on the samples from the posterior distribution are displayed in solid (SERIA_r), broken (SERIA), and dash-dotted (PROSA) lines. Note that data from subject 3 in the PP50 condition is the same as shown in Fig 6. Early outliers are not displayed.

<https://doi.org/10.1371/journal.pcbi.1005692.g008>

four separate ANOVA tests, which revealed that PP had a significant effect on all four units: early unit ($F_{2,138} = 9.2, p < 10^{-3}$), late antisaccade ($F_{2,138} = 26.6, p < 10^{-3}$), late prosaccade ($F_{2,138} = 19.6, p < 10^{-3}$), and inhibitory unit ($F_{2,138} = 30.9, p < 10^{-3}$). We then explored the differences across conditions through planned post hoc tests on each condition for each of the units (Table 6). The arrival times of the early unit did not change significantly between condition PP20 and PP50, but decreased significantly in the PP80 condition as compared to the PP50 block. The response times of late antisaccades increased significantly between the PP20 and the PP50 conditions but not so between the PP50 and PP80. Late prosaccades followed the opposite pattern, showing only a significant decrease in response time between the PP50 and PP80 conditions. Finally, the inhibitory unit changed significantly across all conditions.

Finally, we examined how the probability of a late antisaccade $p(U_a > U_p)$ (Fig 12, right) depended on PP and TT. The estimated parameters for both pro- and antisaccade trials were analyzed with a model with factors SUBJECT, TT, PP and the interaction between TT and PP. An ANOVA test demonstrated that both PP ($F_{2,276} = 51.2, p < 10^{-3}$) and TT ($F_{1,276} = 985.0, p < 10^{-3}$) had a significant effect, but there was no evidence for an interaction between the two factors ($F_{2,276} = 1.5, p < 0.23$), suggesting that PP affected the probability of a late antisaccade equally in pro- and antisaccade trials.

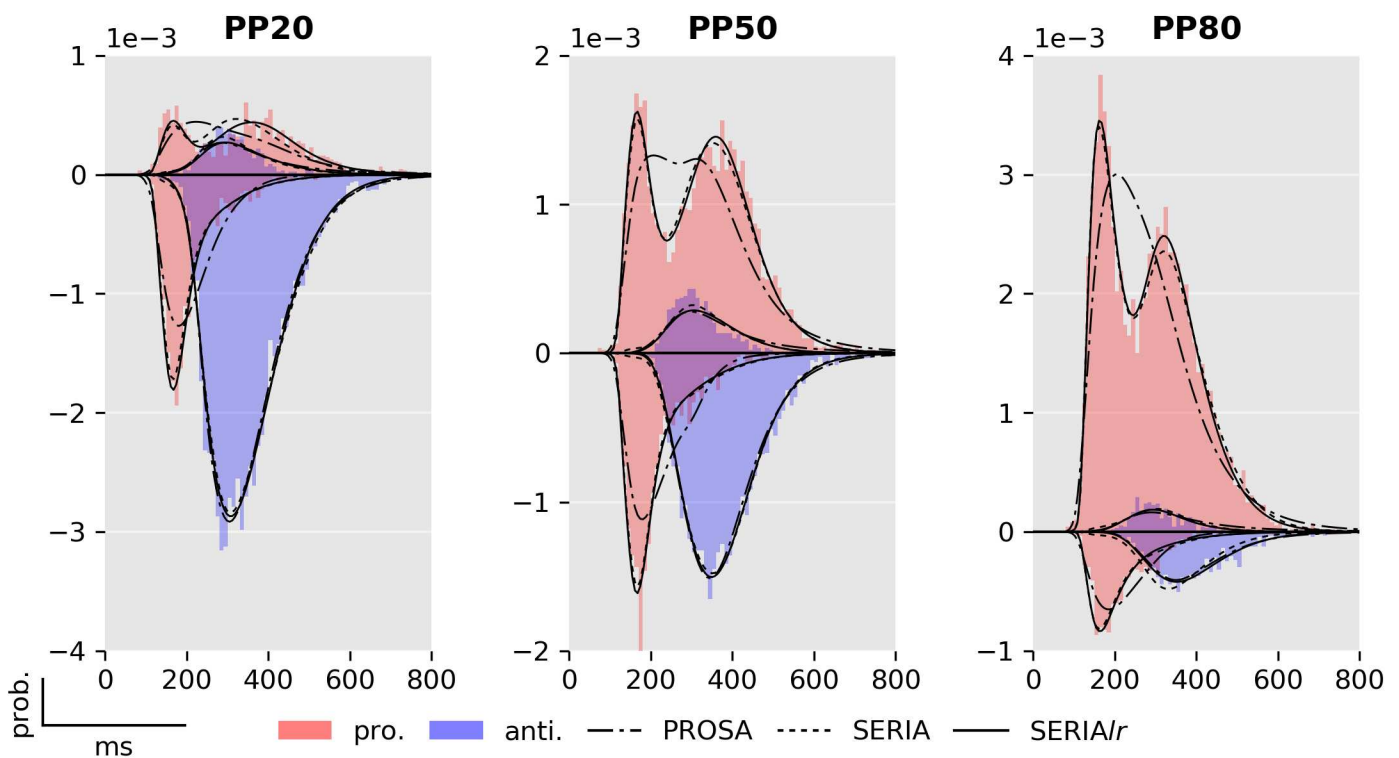


Fig 9. Fits from the best models in each family (m_1, m_8, m_{13}). Model fits and RT histograms for each condition collapsed across subjects. For more details see Figs 6 and 8.

<https://doi.org/10.1371/journal.pcbi.1005692.g009>

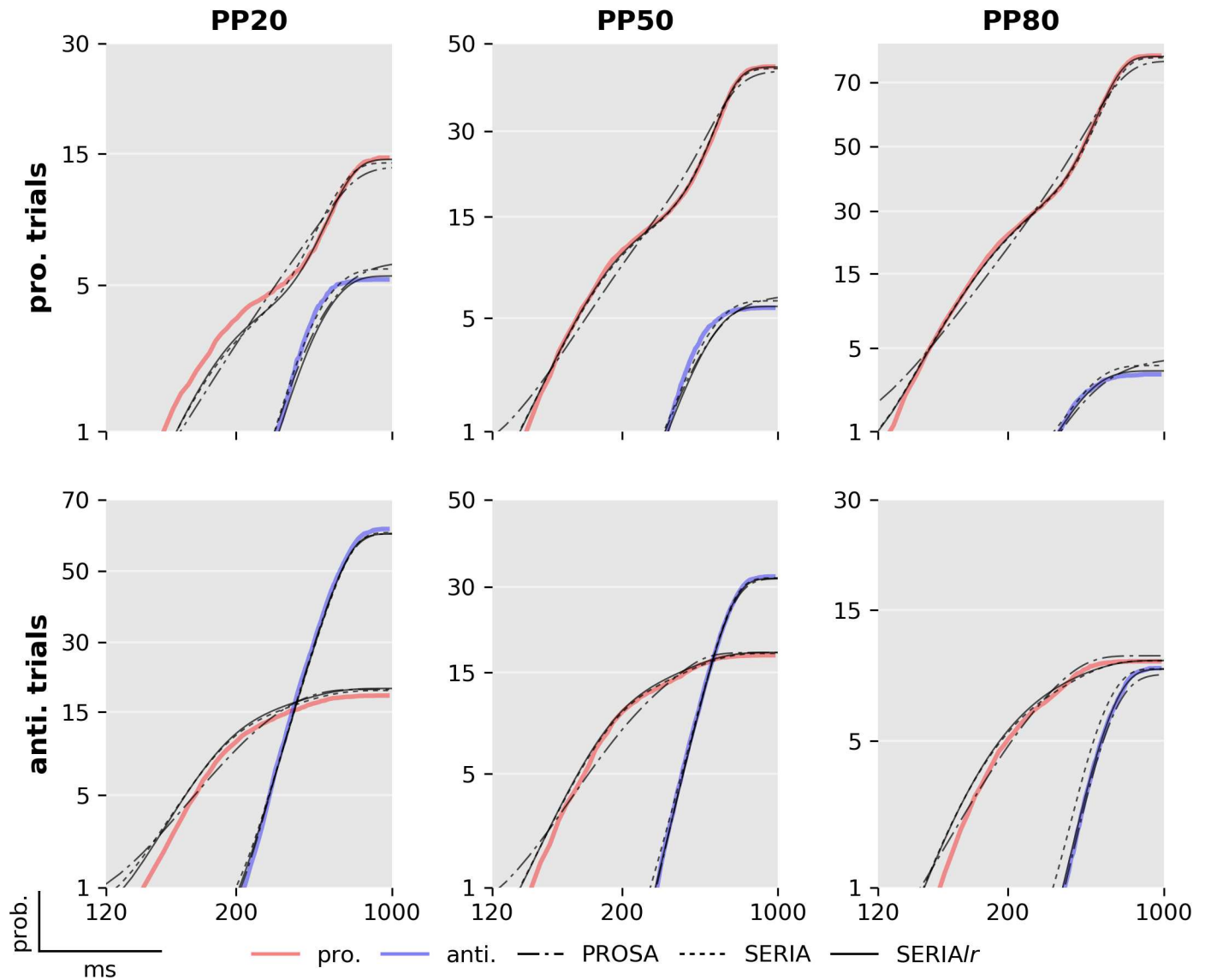


Fig 10. Reciprobit plot of best models. Predicted and empirical cumulative density function of the reciprocal RT in the probit scale for each condition and model collapsed across all subjects. The data shown are the same as in Fig 9, but split for trial types and illustrated as cumulative distributions. Note that the y-axis is in the probit scale and that nearly all differences between the model and the data occur at very small probability values of 5% or below.

<https://doi.org/10.1371/journal.pcbi.1005692.g010>

Subject specific parameters

Finally, we investigated how some of the parameters of the model were related to each other across subjects. Because it has been commonly reported that schizophrenia is related with higher ER, but also with increased antisaccade RT, an interesting question is whether higher late-action response times are correlated with the percentage of late errors and inhibition failures, i.e., early saccades that are not stopped. We found that the response time of late pro ($F_{1,135} = 13.6, p < 0.001$) and antisaccades ($F_{1,135} = 7.1, p < 0.01$) was negatively correlated with the probability of a late error (Fig 13), but no significant interaction between PP and response time was found (pro: $F_{2,135} = 1.7, p = 0.19$; anti: $F_{2,135} = 0.3, p = 0.76$). Hence, late responders tended to make fewer late errors, suggesting a speed/accuracy trade-off in addition to the main effect of PP. We further considered the question whether the percentage of

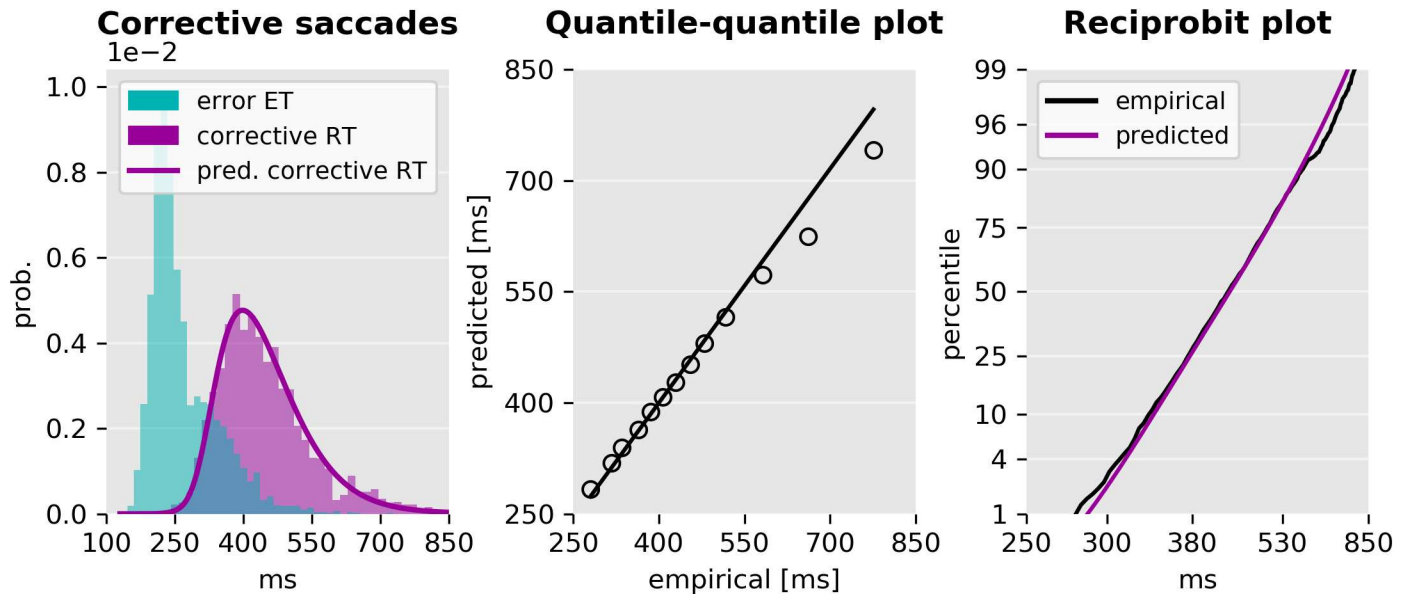


Fig 11. Empirical and predicted RT of corrective antisaccades. Left: End time of erroneous prosaccades, RTs of corrective antisaccades, and time shifted predicted response time distribution of late antisaccades. The time shift was selected to be the difference between the empirical and predicted mean response time. Center: Quantile-quantile plot of the predicted and empirical distribution of corrective antisaccades, and a linear fit to the central 98% quantiles. There is a small deviation only at the tail of the distribution. Right: Reciprobit plot of the empirical and predicted cumulative density functions of the RT of corrective antisaccades. The scale of the horizontal axis is proportional to the reciprocal RT. The vertical axis is in the probit scale.

<https://doi.org/10.1371/journal.pcbi.1005692.g011>

inhibition failures was correlated with the expected arrival time of the late antisaccade unit in antisaccade trials (Fig 13 right). Note that the number of inhibition failures is the same in both trial types in a constrained model, but inhibition failures are errors in antisaccade trials and correct early reactions in prosaccade trials. We found that these parameters were not

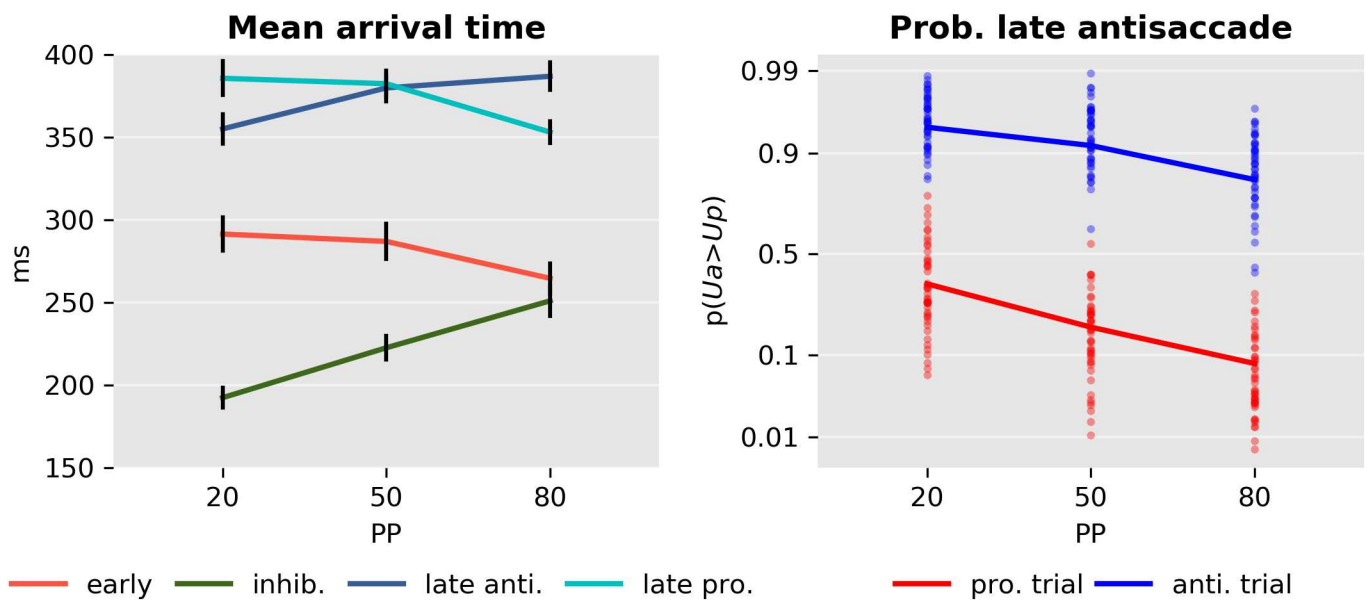


Fig 12. Model parameters. Left: Mean arrival or response time and standard error of the early and inhibitory units and late pro- and antisaccades. Right: Probability of a late antisaccade $p(U_a > U_p)$ in prosaccade (red) and antisaccade (blue) trials in each condition in the probit scale.

<https://doi.org/10.1371/journal.pcbi.1005692.g012>

Table 6. Post hoc comparison of the effect of PP.

	Early			Inhib.			Late pro.			Late anti.		
	Mean [ms]	t_{138}	p	Mean [ms]	t_{138}	p	Mean [ms]	t_{138}	p	Mean [ms]	t_{138}	p
PP20–PP50	4	0.6	0.50	-30	-4.0	<0.001*	3	0.5	0.55	-24	-36	<0.001*
PP20–PP80	26	3.9	<0.001*	-58	-7.8	<0.001*	32	5.7	<0.001*	-32	-5.4	<0.001*
PP50–PP80	22	3.3	0.001*	-28	-3.8	<0.001*	29	5.1	<0.001*	-7	-1.5	0.13

Effect of PP on the mean arrival time of the early and inhibitory unit, and for late pro- and antisaccade units in the corresponding trial type.

*, $p < 0.05$ of a two-tailed t-test.

<https://doi.org/10.1371/journal.pcbi.1005692.t006>

significantly correlated ($F_{2,135} = 1.2, p = 0.26$). This was also the case when we considered the expected response time of late prosaccades in prosaccade trials (not displayed; $F_{2,135} = 0.0, p = 0.98$).

Fig 14 illustrates the posterior distribution of late errors and inhibition failures of two representative subjects as estimated using MCMC. Clearly, PP induced strong differences in the percentage of inhibition failures and late errors in prosaccade trials in both subjects. The effect of PP is less pronounced in late errors in antisaccade trials. The posterior distributions also illustrate how the SERIA_{lr} model can capture individual differences: For example, the percentage of late prosaccade errors in the PP80 condition and the percentage of inhibition failures across all conditions are clearly different in each subject.

Discussion

In this study, we provided a formal treatment of error rates (ER) and reaction times (RT) in the antisaccade task using probabilistic models. We applied these models to data from an experiment consisting of 3 mixed blocks with different probabilities of pro- and antisaccades trials. Model comparison showed that a novel model that allows for late pro- and antisaccades

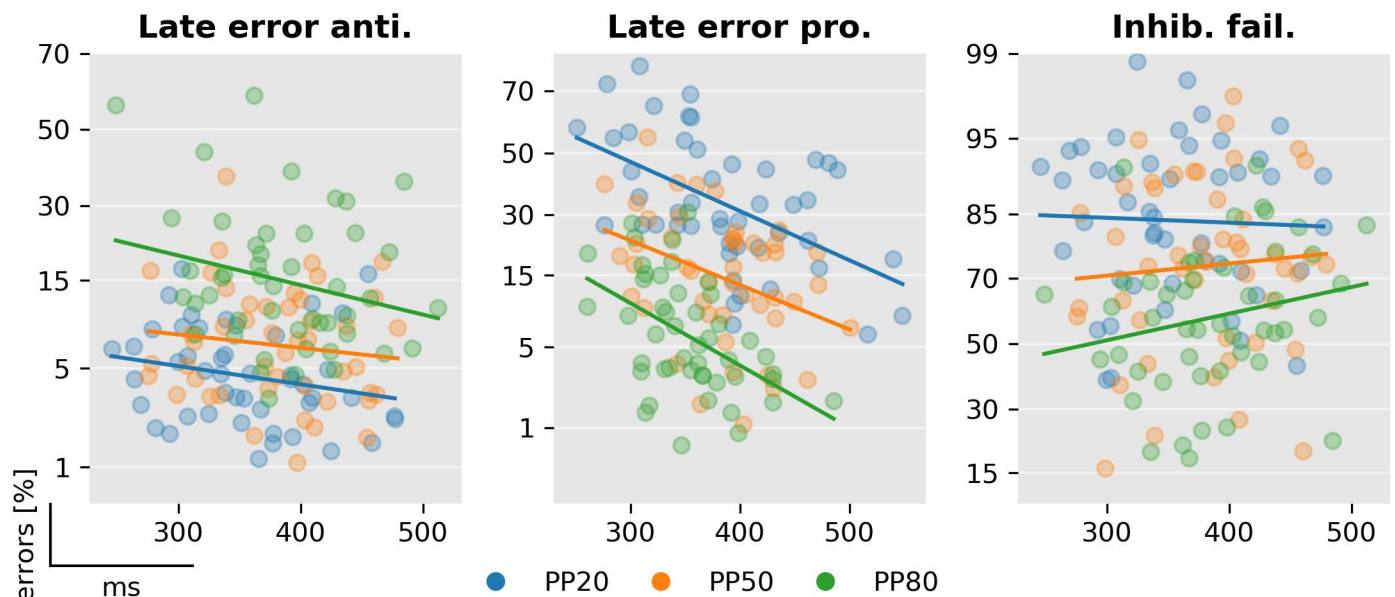


Fig 13. Correlation between late arrival times and errors. Left: Percentage of late errors against late antisaccades' response times in antisaccade trials. Center: Percentage of late errors against late prosaccades' response time in prosaccade trials. Left: Percentage of inhibitory failures against late antisaccades' response time in antisaccade trials. The vertical axis is in the probit scale.

<https://doi.org/10.1371/journal.pcbi.1005692.g013>

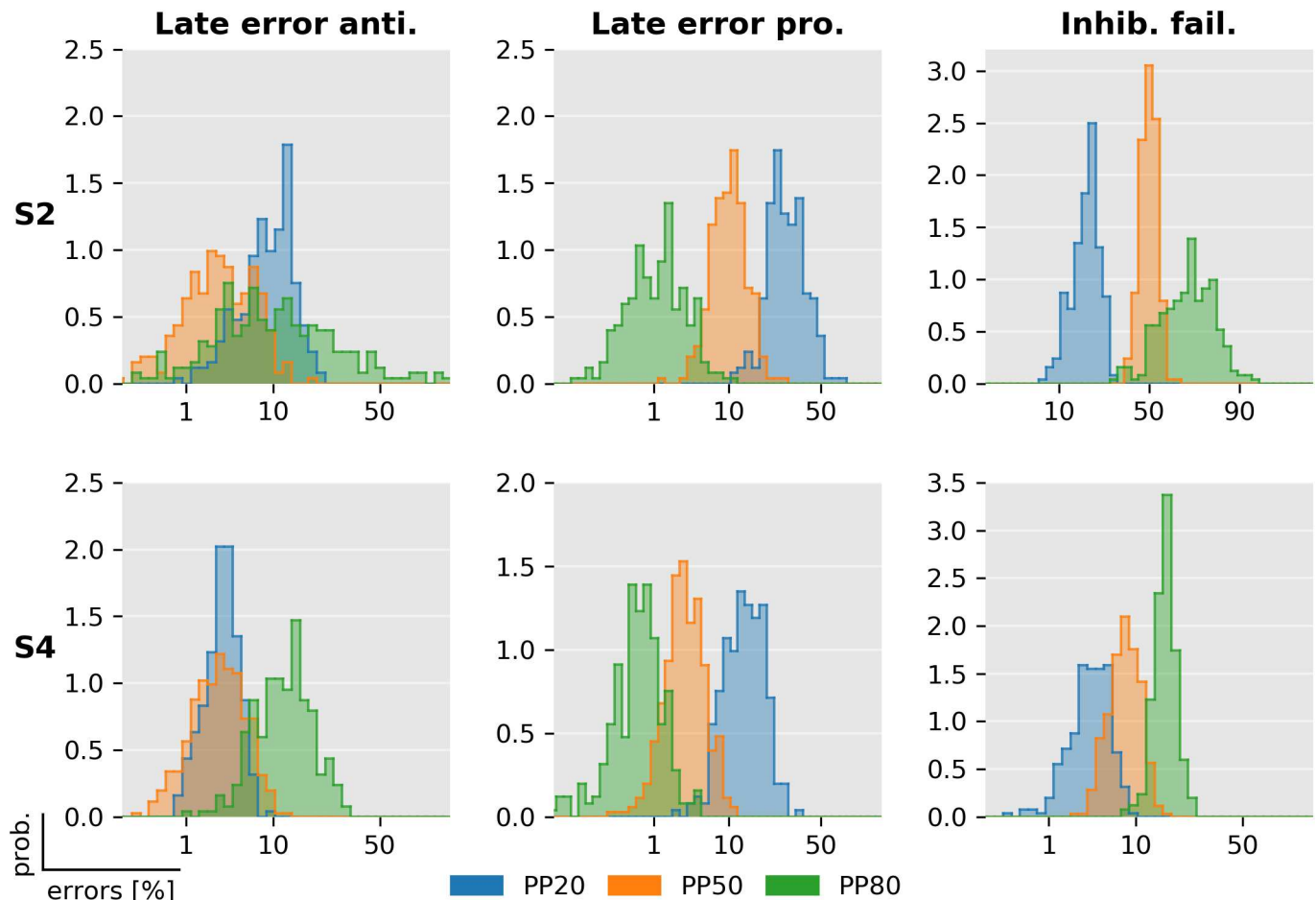


Fig 14. Posterior distribution of late errors and inhibition failures. The posterior distribution of the percentage of late and inhibition failures of two exemplary subjects (see Figs 8 and 13). Samples from the posterior distribution were obtained using MCMC. Histograms display the distributions of the samples in probit scale (horizontal axis). For these two subjects, the posterior distribution of late prosaccade and inhibitory failures clearly discriminates between the three PP conditions.

<https://doi.org/10.1371/journal.pcbi.1005692.g014>

explains our experimental findings better than a model in which all late responses are assumed to be antisaccades. The parameter estimates of the hidden units of the model showed that changes in the inhibitory unit and the late decision process explained most of the overt changes in behavior caused by our experimental manipulation, i.e., differences in trial type probability. Moreover, we found that all units were sensitive to the PP in a block, although late responses tended to plateau when the corresponding trial type was not highly frequent.

Our main finding is that two decision processes are necessary to properly model the anti-saccade task: on one hand, an early race between a prepotent response towards a target and an endogenously generated signal to cancel this action, and, on the other hand, a secondary late race between two units encoding the cue-action mapping. Although the late decision process can be closely approximated by assuming that RT and actions are independent (at least in our experimental design), Bayesian model comparison demonstrated that late decisions are more accurately described by a race between two units representing different actions. The two decision processes are the sources of early errors—fast prosaccades in antisaccade trials— and late errors—late actions incongruent with the cue presented. The late decision process displays a speed/accuracy tradeoff and is biased by the probability of a trial type in a block. Moreover,

this decision process predicts the RT distribution of corrective antisaccades that follow early errors. Because the extra latency of these corrective antisaccades (80ms) is relatively short, it is unlikely that corrective antisaccades are due to a restart in the decision process. Rather these are late actions that overwrite early errors.

Influence of trial type probability on reaction times and error rates

Our results show that both RT and ER depend on PP. While this was a highly significant factor in our study, there are mixed findings in previous reports. ER in antisaccade trials was found to be correlated with TT probability in several studies [29,46,47]. However, this effect might depend on the exact implementation of the task [47,48]. Changes in prosaccade ER similar to our study have been reported by [29] and [48]. Studies in which the type of saccade was signaled at fixation prior to the presentation of the peripheral cue do not always show this effect [47]. The results on RTs are less consistent in the literature. Our findings of increased anti- and decreased prosaccade RTs with higher PP are in line with the overall trend in [29], and with studies in which the cue was presented centrally [47]. Often, there is an additional increase in RT in the PP50 condition [29,47], which was visible in our data as a slight increase in RT in the PP50 condition on top of the linear effect of PP. Overall, RTs in our study were relatively slow compared to studies in which the TT cue was separated from the spatial cue [46,47]. However, a study with a similar design and added visual search reported even slower RTs in both pro- and antisaccades [29].

Interpretation of model comparison results

Formal comparison of generative models can offer insight into the mechanisms underlying eye movement behavior [11] and might be relevant in translational neuromodeling applications, such as computational psychiatry [49–53]. Here, we have presented what is, to our knowledge, the first formal statistical comparison of models of the antisaccade task. For this, we formalized the model introduced in [17] and proceeded to develop a novel model that relaxes the one-to-one association of early and late responses with pro- and antisaccades, respectively. All models and estimation techniques presented here are openly available under the GPLv3.0 license as part of the open source package TAPAS (www.translationalneuromodeling.org/tapas).

Bayesian model comparison yielded four conclusions at the family level. First, the SERIA models were clearly favored when compared to the PROSA models. Second, including a late race between actions representing late pro- and antisaccades (SERIA_{lr}) resulted in an increase in model evidence, compared to a model not including a late race (SERIA). Third, models in which the race parameters of the early and inhibitory unit were constrained to be equal across TT had a higher LME than models in which all parameters were free. Hence, the effect of the cue in a single trial was limited to the late action, and did not affect the race between an early and inhibitory process. This constitutes an important external validation, as it means that model comparison does favor a model which respects the temporal order of the experiment: Information about TT is only available after the stimulus was presented and, thus, it is unlikely to have an impact on fast reactive responses. Fourth, early responses were nearly always prosaccades. Crucially, these four conclusions are based on family-wise comparison across all parametric distribution of the increase rate of the units.

A further consequence of our findings is that two independent and qualitatively different decision processes lead to an antisaccade: the race process between early and inhibitory units, and the secondary decision process that generates late responses. A separation of decisions into a ‘where’ and a ‘when’ component has been proposed by [54], but mainly in conceptual

terms. However, model comparison showed that these two components (‘where’ and ‘when’) cannot be completely dissociated and that time plays a role in late decisions. Nevertheless, the assumption that action type and arrival time of late responses were independent yielded a good fit to this particular data set, suggesting that it is, in many cases, an acceptable approximation to assume a time-independent late decision process. The most obvious difference between the SERIA and SERIA_{lr} can be observed in prosaccade trials in the PP20 condition (left panel, upper half plane Fig 9), in which late prosaccades are slower than antisaccades. We discuss this point in more detail below.

Parametric distribution of reaction times. The parametric distribution of oculomotor RTs has been discussed in great detail in the literature (e.g., [13,55]). Here, we did not aim at determining the most suitable distribution, but rather opted for a practical approach by evaluating different models with a reduced number of parametric distributions. We then based our conclusions on the model with the highest LME. Nevertheless, one can consider the connection of the models presented here with other families of parametric distributions. In particular, the linear relationship

$$\frac{s_i}{r_i} = t \tag{38}$$

could be seen as formally inconsistent with the observation that RT are likely to be explained by stochastic accumulation processes (see for example [56,57], but [58]). This is a weaker constraint than one would expect, because under low noise conditions, for example, a linear relationship can be a good approximation of neural activity. Even if the relationship is not linear, for any continuous function ϕ with an inverse function ϕ^{-1} , the model can be recasted as [59]:

$$s_i = \phi(tr_i), \tag{39}$$

$$\frac{\phi^{-1}(s_i)}{r_i} = t. \tag{40}$$

In any case, linear accumulation models have been shown to yield similar conclusions to stochastic accumulation models [58].

More generally, it can be shown that if RTs follow a generalized inverse normal distribution (GIN) of the form

$$GIN(t; \lambda, \kappa, \psi) = \frac{\left(\frac{\psi}{\kappa}\right)^\lambda}{2K_\lambda(\sqrt{\kappa\psi})} t^{\lambda-1} \exp\left(-\frac{1}{2}(\kappa t^{-1} + \psi t)\right) \tag{41}$$

where $\lambda \leq 0$, and K_λ is a modified Bessel function of the second kind, there exists a continuous diffusion process whose first hit distribution (FHD) follows the GIN [60]. A particular case of this distribution is the Wald distribution for which $\lambda = -\frac{1}{2}$, $\kappa = 0$. It is the FHD of the Brownian diffusion process with drift

$$X_t = -\sqrt{\sigma}\psi t + \sigma W_t \tag{42}$$

where W_t denotes a Wiener process, $x_0 > 0$, and the absorbing boundary a is zero. More relevant here, when $\psi = 0$ the distribution reduces to an inverse gamma distribution, the FHD of the process

$$X_t = \sqrt{\sigma}(2\lambda - 1)t^{-1} + \sigma W_t \tag{43}$$

with $x_0 > 0$ and boundary $a = 0$ (for a detailed mathematical treatment see [60]). Thus, if the rates of a ballistic, linear processes are assumed to be gamma distributed, the RTs follow a distribution that is formally equivalent to a first hit model with stochastic updates and fixed rates. While the model presented here can be seen as a ballistic accumulation model, this equivalence suggests that it is *compatible* with a diffusion process with infinitesimal mean change proportional to t^{-1} .

Other antisaccade models. In broad terms, three families of antisaccade models can be distinguished (reviewed in [61]). The first set of models is based on a race process with independent saccadic and stop units. These models build on the seminal work of [16] on the stop-signal paradigm. According to this model, a ‘GO’ signal triggers a stochastic ‘race’ process that generates a response once it reaches threshold. Critically, a stop signal triggers a second process that inhibits the first ‘GO’ response if it is the first to reach threshold. Moreover, the rates of both units are assumed to be independent. This model was further extended for the antisaccade task by [17] (but see [14,21], and the review in [20]), who included a third unit such that an antisaccade is generated when a reflexive prosaccade is inhibited by an endogenously-triggered stop process. Note that the original ‘horse-race’ model has also been modified [62] to account for different competing response actions, similarly as in the antisaccade task. The models proposed here belong to this family.

A second type of model relies on lateral or mutual inhibition of competing pro- and anti-saccade units. In this direction, Cutsuridis and colleagues [61,63,64] proposed that lateral inhibition is implemented by inhibitory connections in the intermediate layers of the superior colliculus. Thus, saccades are the result of accumulation processes, but these are not independent of each other. Crucially, no veto-like stop signal is required. Although no formal model-fitting has been proposed for this model, qualitative agreement with data suggests that it might capture behavioral patterns relevant in translational applications [64,65]. Since no probabilistic version of this model is available, it is not yet possible to decide on the grounds of model comparison whether mutually dependent or independent race processes best explain current behavioral findings.

Finally, several models that incorporate detailed physiological mechanisms have been proposed [23,66–68]. These models cannot be easily assigned to one of the above categories, as they often employ both an inhibitory mechanism that stops or withholds the reactive responses as well as competition between actions. In addition, while more realistic models possess a more fine-grained representation of the underlying neurobiology, they rely on a large number of parameters and for this reason, it is difficult to fit them to behavioral data (for discussion, see [11]).

Regarding neurobiologically realistic models, the model proposed by [23] is the most similar to the SERIA model. It posits two different mechanisms that interact in the generation of antisaccades: an action-selection module and a remapping module that controls the cue-action mapping. As a consequence, this model allows for the generation of late errors that follow a similar RT distribution as correct antisaccades. Consistent with this observation, the SERIA model can quantitatively distinguish between inhibition and late cue-action mapping errors (Fig 15, left panel). A less obvious similarity between the SERIA model and [23] is that different cues do not lead *directly* to different dynamics in the action module, but only in the so-called ‘remapping’ module. Furthermore, the incorporation of a late race is conceptually close to the approach proposed by [23], which includes a winner-take-all competition in what we have referred here as late responses. Similarly, our model comparison results show that different cues (i.e., trial types) do not affect the GO/NO-GO process but only the late cue-action mapping.

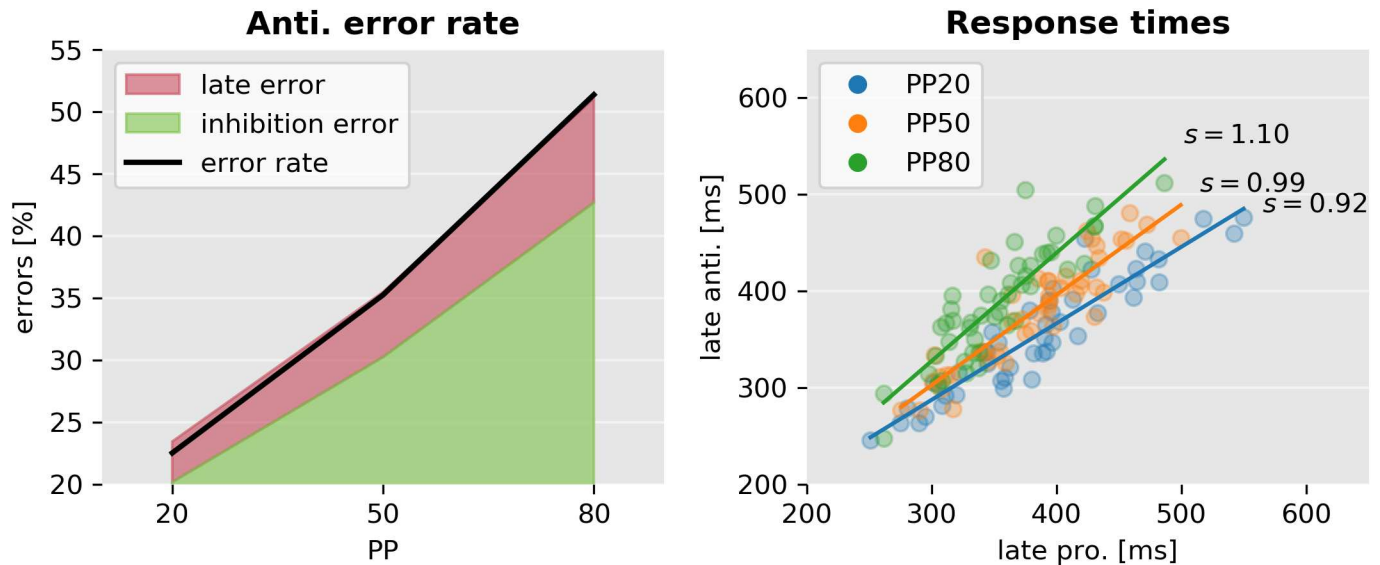


Fig 15. Error sources and the correlation of response times. Left: Error rate (black line) split into the two causes predicted by the model. Inhibition errors are early actions that always trigger prosaccades. Similarly as described by [23], late errors occur when a late response leads to a prosaccade. Right: Correlation between correct antisaccades' and late prosaccades' response times according to the best SERIA_c model. The best linear fit is depicted as a solid line. The mean ratio of pro- and antisaccade response times (s) is displayed on the right. Although late pro- and antisaccade response times are highly correlated, their ratio is different in each condition (interaction PP and late prosaccade response time $F = 9.2$, $p < 0.001$).

<https://doi.org/10.1371/journal.pcbi.1005692.g015>

Parameter changes across trial types

One of the most salient results presented here is that models in which the parameters of the units were constrained to be equal across trial types had a larger LME than models in which all the parameters were free, suggesting that the early and inhibitory race units were not affected by the cue presented in a single trial. While visual inspection of the predicted likelihood under the posterior parameters showed that most of the prominent characteristics of the data were explained correctly, some more subtle effects were not captured accurately by the SERIA model. This is particularly clear in the PP20 condition, in which the SERIA model displays a large bias in prosaccades trials in the PP20 condition. One possible explanation is that restricting the parameters across trial types made the model too rigid to capture this effect. Fig 16 compares the fitted RT distributions for models m_8 (SERIA) and m_{13} (SERIA_{lr}), in which no constraint on the parameters was imposed. Both models are qualitatively almost identical, although as shown in Fig 7, the LME favored the SERIA_{lr} model. Thereby, the qualitative similarity between both models indicates that, in our experiment, the RT of late decisions is only weakly dependent on time. In conclusion, although removing the constraint on the parameters did improve the fit, the differences are marginal and thus did not justify the additional model complexity. As mentioned above this is consistent with the notion that the information about trial type is only available to a subject once the peripheral stimulus (green bar) has been processed, presumably tens of milliseconds after the stimulus onset. In fact, this example illustrates the protection against overfitting provided by the LME, as this is a case in which simpler models were preferred over more complex models despite of slightly less accurate fits.

Arguably, the constrained SERIA model fails to fully capture the RT of late prosaccade in the PP20 and PP50 conditions because of the assumption that late prosaccades have the same arrival time as late antisaccades. As shown in Fig 15, although the response time of late pro-

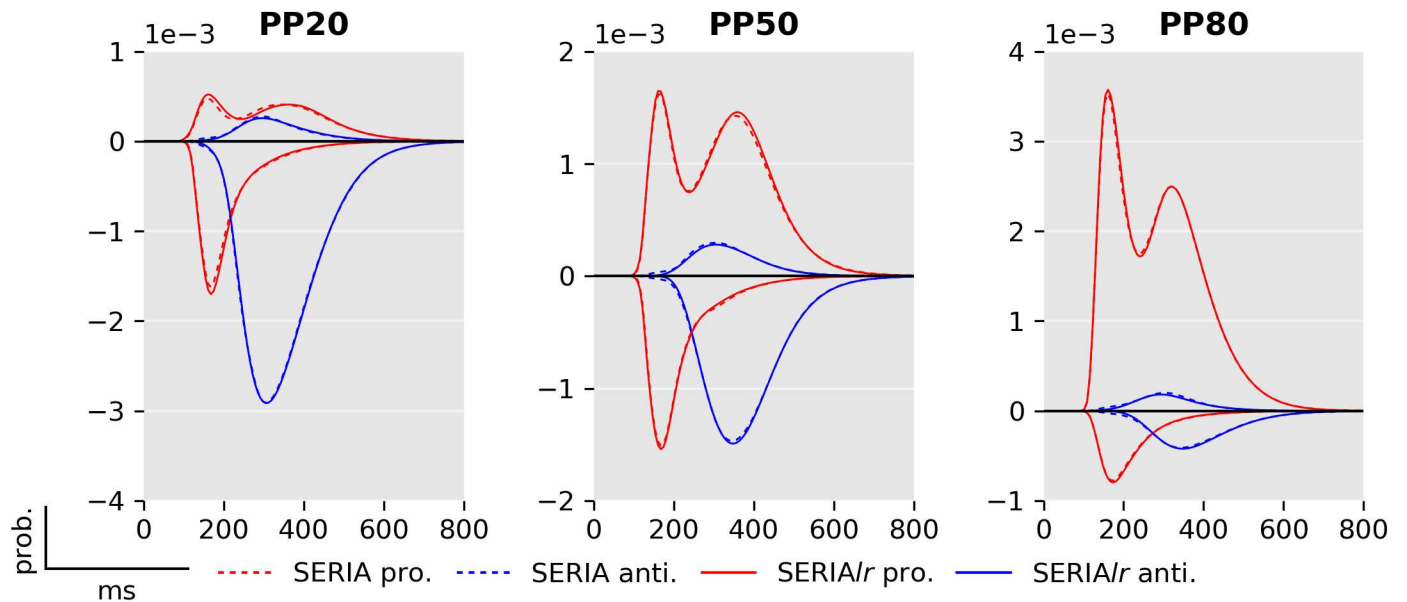


Fig 16. Comparison between unconstrained SERIA and SERIA_{Ir} models. Comparison between models m_8 (broken lines; SERIA model) and m_{13} (solid lines; late race SERIA_{Ir} model).

<https://doi.org/10.1371/journal.pcbi.1005692.g016>

and antisaccades are strongly correlated, the average ratio of the response times changes across conditions.

The effect of trial type probability

It is far from obvious why TT probability affects RT and ER in the antisaccade task. One possible explanation is that increased probability leads to higher preparedness for either pro- or antisaccades. Such a theory posits an intrinsic trade-off between preparations for one of the two action types that leads to higher RTs and ERs in low probability trials. Thus, a trade-off theory predicts that the arrival times of early and late responses should be negatively correlated. Although this hypothesis can explain our behavioral findings in terms of summary statistics, our model suggests a more complicated picture.

The main explanation of our results is the effect of TT probability on the inhibitory unit and the probability of a late prosaccade. A higher probability of antisaccade trials leads to faster inhibition and to a higher number of late prosaccades. This resulted in higher mean RT in prosaccade trials when PP is low. In the case of antisaccades, although the mean arrival times of the late unit increased in the PP50 condition, the increased arrival time of the inhibitory unit on the PP80 condition skewed the antisaccade distribution towards higher RTs. Nevertheless, the SERIA_{Ir} implies the anticorrelation of late pro- and antisaccades in a single trial type, as these are the results of a GO-GO race.

Action inhibition

The biological implementation of action inhibition in the antisaccade and other countermanding tasks has received a lot of attention and is still debated [69–73]. Our work adds evidence to the theory that the antisaccade task requires a process that inhibits prepotent responses and is independent of the initiation of a late action [20]. Recent evidence from electrophysiological recordings in the rat brain ([74] reviewed by [71]) suggests that the hypothesized race between

GO and inhibitory responses might be implemented by different pathways in the basal ganglia [68]. In addition to the basal ganglia, microstimulation of the supplementary eye fields tends to facilitate inhibition of saccades in the countermanding task [75].

Corrective antisaccades

Although not a primary goal of our model, we considered the question of predicting corrective antisaccades. This problem has received some attention recently [18,61,65,76], as more sophisticated models of the antisaccade task have been developed. We speculated that corrective antisaccades are generated by the same mechanism as late responses. Thus, their RT distribution should follow a similar distribution. Our results strongly suggest that this is the case (see Fig 11). Moreover, the time delay of the corrective antisaccades indicates that, on average, these actions are not the result of the late unit being restarted at the end time of the erroneous prosaccade, as this would lead to much higher RTs. Rather, the planning of a corrective antisaccade might be started much before the end of the execution of an erroneous prosaccade, in accordance with the parallel planning model of the antisaccade task [46] and the ‘GO–STOP +GO’ model in [21].

Translational applications

Despite the large number of studies of clinical patients using the antisaccade task, an important question remains open: What are the causes of the errors in different neurological and psychiatric conditions? For example [77,78] argued that errors in schizophrenia might be explained, at least partially, by a failure to generate a secondary late action based on several modifications of the antisaccade task. However, it was also proposed that the increased ER in schizophrenia is due to high tonic dopamine levels in the basal ganglia, that lead to decreased inhibition of early responses [68]. More generally, different neurological and psychiatric diseases, or even patients with the same condition, might be characterized by a different source of errors. For example, there is intriguing evidence [79] that patients with different diseases such as attention deficits disorders [80], Parkinson’s disease [81], and amyotrophic lateral sclerosis [82] might be characterized by different ratios of early and late errors. An interesting experimental finding in our study related to this is the considerable amount of erroneous antisaccades in prosaccade trials. An increased number of such errors could be caused by reduced cognitive flexibility leading to impaired shifting between tasks as observed for example in obsessive compulsive disorder [83]. The ability to quantify different types of errors through computational modeling might help to further characterize these diseases.

Summary

Here we have presented a novel model of the antisaccade task. While the basic structure of the model follows the layout of a previous model [17], we have introduced two crucial advancements. First, we postulated that late responses could trigger both pro- and antisaccades, which are selected by an independent decision process. Second, the generative nature of our model allows for Bayesian model inversion, which enables the comparison of different models and families of models on formal grounds. To our knowledge this has not been done for any of the previous models of the antisaccade task, which is of relevance for translational applications that aim at better understanding psychiatric diseases by means of computational modeling.

The application of the model to a large data set yielded several novel results. First, the early and inhibitory race processes triggered by different cues are almost identical. Moreover, different PP had very different effects on the individual units, which was not obvious from the linear analysis of the mean RT and ER. Crucially, our modeling approach allowed us to look at a

mechanistic explanation or the effects of PP by examining the individual units. In future work we aim to disentangle the mechanisms of behavioral differences caused by neuromodulatory drugs and psychiatric illnesses using formal Bayesian inference.

Supporting information

S1 Dataset. Table of data. Spreadsheet including all reaction times, actions and errors that entered the analysis. More details are included in the file.
(XLSM)

S1 Fig. Reaction time and error rate in all conditions for each subject. Mean reaction times and error rates are displayed as solid lines.
(TIFF)

Acknowledgments

We thank Saeed Paliwal for her remarks and helpful comments on an earlier version of this manuscript.

Author Contributions

Conceptualization: Eduardo A. Aponte, Dario Schöbi, Klaas E. Stephan, Jakob Heinzle.

Data curation: Eduardo A. Aponte.

Formal analysis: Eduardo A. Aponte, Jakob Heinzle.

Funding acquisition: Klaas E. Stephan.

Investigation: Eduardo A. Aponte.

Methodology: Eduardo A. Aponte, Dario Schöbi, Jakob Heinzle.

Project administration: Jakob Heinzle.

Resources: Klaas E. Stephan.

Software: Eduardo A. Aponte, Dario Schöbi.

Supervision: Jakob Heinzle.

Visualization: Eduardo A. Aponte, Jakob Heinzle.

Writing – original draft: Eduardo A. Aponte, Jakob Heinzle.

Writing – review & editing: Eduardo A. Aponte, Dario Schöbi, Klaas E. Stephan, Jakob Heinzle.

References

1. Hallett PE. Primary and secondary saccades to goals defined by instructions. *Vision Res.* 1978; 18: 1279–1296. PMID: [726270](https://pubmed.ncbi.nlm.nih.gov/726270/)
2. Munoz DP, Everling S. Look away: the anti-saccade task and the voluntary control of eye movement. *Nat Rev Neurosci.* 2004; 5: 218–228. <https://doi.org/10.1038/nrn1345> PMID: [14976521](https://pubmed.ncbi.nlm.nih.gov/14976521/)
3. Hutton SB, Ettinger U. The antisaccade task as a research tool in psychopathology: a critical review. *Psychophysiology.* 2006; 43: 302–313. <https://doi.org/10.1111/j.1469-8986.2006.00403.x> PMID: [16805870](https://pubmed.ncbi.nlm.nih.gov/16805870/)
4. Fukushima J, Fukushima K, Chiba T, Tanaka S, Yamashita I, Kato M. Disturbances of voluntary control of saccadic eye movements in schizophrenic patients. *Biol Psychiatry.* 1988; 23: 670–677. PMID: [3370264](https://pubmed.ncbi.nlm.nih.gov/3370264/)

5. Curtis CE, Calkins ME, Grove WM, Feil KJ, Iacono WG. Saccadic disinhibition in patients with acute and remitted schizophrenia and their first-degree biological relatives. *Am J Psychiatry*. 2001; 158: 100–106. <https://doi.org/10.1176/appi.ajp.158.1.100> PMID: 11136640
6. Harris MS, Reilly JL, Keshavan MS, Sweeney JA. Longitudinal studies of antisaccades in antipsychotic-naïve first-episode schizophrenia. *Psychol Med*. 2006; 36: 485–494. <https://doi.org/10.1017/S0033291705006756> PMID: 16388703
7. Reilly JL, Frankovich K, Hill S, Gershon ES, Keefe RS, Keshavan MS, et al. Elevated antisaccade error rate as an intermediate phenotype for psychosis across diagnostic categories. *Schizophr Bull*. 2014; 40: 1011–1021. <https://doi.org/10.1093/schbul/sbt132> PMID: 24080895
8. Radant AD, Millard SP, Braff DL, Calkins ME, Dobie DJ, Freedman R, et al. Robust differences in anti-saccade performance exist between COGS schizophrenia cases and controls regardless of recruitment strategies. *Schizophr Res*. 2015; 163: 47–52. <https://doi.org/10.1016/j.schres.2014.12.016> PMID: 25553977
9. Crawford TJ, Sharma T, Puri BK, Murray RM, Berridge DM, Lewis SW. Saccadic eye movements in families multiply affected with schizophrenia: the Maudsley Family Study. *Am J Psychiatry*. 1998; 155: 1703–1710. <https://doi.org/10.1176/ajp.155.12.1703> PMID: 9842779
10. Radant AD, Dobie DJ, Calkins ME, Olincy A, Braff DL, Cadenhead KS, et al. Antisaccade performance in schizophrenia patients, their first-degree biological relatives, and community comparison subjects: data from the COGS study. *Psychophysiology*. 2010; 47: 846–856. <https://doi.org/10.1111/j.1469-8986.2010.01004.x> PMID: 20374545
11. Heinzle J, Aponte EA, Stephan KE. Computational models of eye movements and their application to schizophrenia. *Current Opinion in Behavioral Sciences*. 2016; 11: 21–29. <https://doi.org/https://doi.org/10.1016/j.cobeha.2016.03.008>
12. Wolfe JM, Palmer EM, Horowitz TS. Reaction time distributions constrain models of visual search. *Vision Res*. 2010; 50: 1304–1311. <https://doi.org/10.1016/j.visres.2009.11.002> PMID: 19895828
13. Palmer EM, Horowitz TS, Torralba A, Wolfe JM. What are the shapes of response time distributions in visual search? *J Exp Psychol Hum Percept Perform*. 2011; 37: 58–71. <https://doi.org/10.1037/a0020747> PMID: 21090905
14. Noorani I, Carpenter RH. Full reaction time distributions reveal the complexity of neural decision-making. *Eur J Neurosci*. 2011; 33: 1948–1951. <https://doi.org/10.1111/j.1460-9568.2011.07727.x> PMID: 21645090
15. Huys QJ, Maia TV, Frank MJ. Computational psychiatry as a bridge from neuroscience to clinical applications. *Nat Neurosci*. 2016; 19: 404–413. <https://doi.org/10.1038/nn.4238> PMID: 26906507
16. Logan GD, Cowan WB, Davis KA. On the ability to inhibit simple and choice reaction time responses: a model and a method. *J Exp Psychol Hum Percept Perform*. 1984; 10: 276–291. PMID: 6232345
17. Noorani I, Carpenter RH. Antisaccades as decisions: LATER model predicts latency distributions and error responses. *Eur J Neurosci*. 2013; 37: 330–338. <https://doi.org/10.1111/ejn.12025> PMID: 23121177
18. Noorani I, Carpenter RH. Re-starting a neural race: anti-saccade correction. *Eur J Neurosci*. 2014; 39: 159–164. <https://doi.org/10.1111/ejn.12396> PMID: 24168375
19. Noorani I. LATER models of neural decision behavior in choice tasks. *Front Integr Neurosci*. 2014; 8: 67. <https://doi.org/10.3389/fnint.2014.00067> PMID: 25202242
20. Noorani I. Towards a unifying mechanism for cancelling movements. *Philos Trans R Soc Lond, B, Biol Sci*. 2017; 372.
21. Camalier CR, Gotler A, Murthy A, Thompson KG, Logan GD, Palmeri TJ, et al. Dynamics of saccade target selection: race model analysis of double step and search step saccade production in human and macaque. *Vision Res*. 2007; 47: 2187–2211. <https://doi.org/10.1016/j.visres.2007.04.021> PMID: 17604806
22. Carpenter RH, Williams ML. Neural computation of log likelihood in control of saccadic eye movements. *Nature*. 1995; 377: 59–62. <https://doi.org/10.1038/377059a0> PMID: 7659161
23. Lo CC, Wang XJ. Conflict Resolution as Near-Threshold Decision-Making: A Spiking Neural Circuit Model with Two-Stage Competition for Antisaccadic Task. *PLoS Comput Biol*. 2016; 12: e1005081. <https://doi.org/10.1371/journal.pcbi.1005081> PMID: 27551824
24. Brown SD, Heathcote A. The simplest complete model of choice response time: linear ballistic accumulation. *Cogn Psychol*. 2008; 57: 153–178. <https://doi.org/10.1016/j.cogpsych.2007.12.002> PMID: 18243170
25. Gorea A, Rider D, Yang Q. A unified comparison of stimulus-driven, endogenous mandatory and “free choice” saccades. *PLoS ONE*. 2014; 9: e88990. <https://doi.org/10.1371/journal.pone.0088990> PMID: 24586474

26. Edelman JA, Valenzuela N, Barton JJ. Antisaccade velocity, but not latency, results from a lack of saccade visual guidance. *Vision Res.* 2006; 46: 1411–1421. <https://doi.org/10.1016/j.visres.2005.09.013> PMID: 16260025
27. Zhang M, Barash S. Neuronal switching of sensorimotor transformations for antisaccades. *Nature.* 2000; 408: 971–975. <https://doi.org/10.1038/35050097> PMID: 11140683
28. Sato TR, Schall JD. Effects of stimulus-response compatibility on neural selection in frontal eye field. *Neuron.* 2003; 38: 637–648. PMID: 12765614
29. Chiau HY, Tseng P, Su JH, Tzeng OJ, Hung DL, Muggleton NG, et al. Trial type probability modulates the cost of antisaccades. *J Neurophysiol.* 2011; 106: 515–526. <https://doi.org/10.1152/jn.00399.2010> PMID: 21543748
30. Stampe D. Heuristic filtering and reliable calibration methods for video-based pupil-tracking systems. *Behavior Research Methods, Instruments, & Computers.* Springer-Verlag; 1993; 25: 137–142. <https://doi.org/10.3758/BF03204486>
31. Robert C, Casella G. Monte Carlo statistical methods. Springer Science & Business Media; 2013.
32. Shaby B, Wells MT. Exploring an adaptive Metropolis algorithm. Durham, NC, USA: Department of statistical science. Duke University; 2010.
33. Gelman A, Carlin JB, Stern HS, Rubin DB. Bayesian Data Analysis. Chapman and Hall/CRC; 2003.
34. Aponte EA, Raman S, Sengupta B, Penny WD, Stephan KE, Heinzle J. mpdcm: A toolbox for massively parallel dynamic causal modeling. *J Neurosci Methods.* 2016; 257: 7–16. <https://doi.org/10.1016/j.jneumeth.2015.09.009> PMID: 26384541
35. Ben Calderhead, Girolami MA. Estimating Bayes factors via thermodynamic integration and population MCMC. *Computational Statistics & Data Analysis.* 2009; 53: 4028–4045. <https://doi.org/10.1016/j.csda.2009.07.025>
36. Gelman A, Rubin DB. Inference from iterative simulation using multiple sequences. *Statistical Science.* JSTOR; 1992;: 457–472.
37. MacKay DJC. Information Theory, Inference, and Learning Algorithms. Cambridge University Press; 2003.
38. Stephan KE, Penny WD, Daunizeau J, Moran RJ, Friston KJ. Bayesian model selection for group studies. *Neuroimage.* 2009; 46: 1004–1017. <https://doi.org/10.1016/j.neuroimage.2009.03.025> PMID: 19306932
39. Gelman A, Meng XL. Simulating Normalizing Constants: From Importance Sampling to Bridge Sampling to Path Sampling. *Statistical Science.* Institute of Mathematical Statistics; 1998; 13: 163–185. <https://doi.org/10.2307/2676756>
40. Kass RE, Raftery AE. Bayes factors. *Journal of the American Statistical Association.* Taylor & Francis Group; 1995; 90: 773–795.
41. Rigoux L, Stephan KE, Friston KJ, Daunizeau J. Bayesian model selection for group studies—revisited. *Neuroimage.* 2014; 84: 971–985. <https://doi.org/10.1016/j.neuroimage.2013.08.065> PMID: 24018303
42. Penny WD, Stephan KE, Daunizeau J, Rosa MJ, Friston KJ, Schofield TM, et al. Comparing families of dynamic causal models. *PLoS Comput Biol.* 2010; 6: e1000709. <https://doi.org/10.1371/journal.pcbi.1000709> PMID: 20300649
43. Brodersen KH, Schofield TM, Leff AP, Ong CS, Lomakina EI, Buhmann JM, et al. Generative embedding for model-based classification of fMRI data. *PLoS Comput Biol.* 2011; 7: e1002079. <https://doi.org/10.1371/journal.pcbi.1002079> PMID: 21731479
44. Stephan KE, Schlagenhauf F, Huys QJ, Raman S, Aponte EA, Brodersen KH, et al. Computational neuroimaging strategies for single patient predictions. *Neuroimage.* 2017; 145: 180–199. <https://doi.org/10.1016/j.neuroimage.2016.06.038> PMID: 27346545
45. Patterson TNL. The optimum addition of points to quadrature formulae. *Mathematics of Computation.* 1968; 22: 847–856.
46. Massen C. Parallel programming of exogenous and endogenous components in the antisaccade task. *Q J Exp Psychol A.* 2004; 57: 475–498. <https://doi.org/10.1080/02724980343000341> PMID: 15204137
47. Pierce JE, McDowell JE. Effects of preparation time and trial type probability on performance of anti- and pro-saccades. *Acta Psychol (Amst).* 2016; 164: 188–194.
48. Pierce JE, McDowell JE. Modulation of cognitive control levels via manipulation of saccade trial-type probability assessed with event-related BOLD fMRI. *J Neurophysiol.* 2016; 115: 763–772. <https://doi.org/10.1152/jn.00776.2015> PMID: 26609113
49. Montague PR, Dolan RJ, Friston KJ, Dayan P. Computational psychiatry. *Trends Cogn Sci (Regul Ed).* 2012; 16: 72–80.

50. Wang XJ, Krystal JH. Computational psychiatry. *Neuron*. 2014; 84: 638–654. <https://doi.org/10.1016/j.neuron.2014.10.018> PMID: 25442941
51. Stephan KE, Mathys C. Computational approaches to psychiatry. *Curr Opin Neurobiol*. 2014; 25: 85–92. <https://doi.org/10.1016/j.conb.2013.12.007> PMID: 24709605
52. Paulus MP, Huys QJ, Maia TV. A Roadmap for the Development of Applied Computational Psychiatry. *Biological Psychiatry: Cognitive Neuroscience and Neuroimaging*. Elsevier; 2016.
53. Huys QJ, Maia TV, Paulus MP. Computational Psychiatry: From Mechanistic Insights to the Development of New Treatments. *Biological Psychiatry: Cognitive Neuroscience and Neuroimaging*. Elsevier; 2016; 1: 382–385.
54. Findlay JM, Walker R. A model of saccade generation based on parallel processing and competitive inhibition. *Behav Brain Sci*. 1999; 22: 661–674. PMID: 11301526
55. Feng G. Is there a common control mechanism for anti-saccades and reading eye movements? Evidence from distributional analyses. *Vision Res*. 2012; 57: 35–50. <https://doi.org/10.1016/j.visres.2012.01.001> PMID: 22260785
56. Gold JI, Shadlen MN. The neural basis of decision making. *Annu Rev Neurosci*. 2007; 30: 535–574. <https://doi.org/10.1146/annurev.neuro.29.051605.113038> PMID: 17600525
57. Ratcliff R, Smith PL, Brown SD, McKoon G. Diffusion Decision Model: Current Issues and History. *Trends Cogn Sci (Regul Ed)*. 2016; 20: 260–281.
58. Donkin C, Brown S, Heathcote A, Wagenmakers EJ. Diffusion versus linear ballistic accumulation: different models but the same conclusions about psychological processes? *Psychon Bull Rev*. 2011; 18: 61–69. <https://doi.org/10.3758/s13423-010-0022-4> PMID: 21327360
59. Moscoso del Prado Martin F. A theory of reaction time distributions. 2008.
60. Barndorff-Nielsen O, Blæsild P, Halgreen C. First hitting time models for the generalized inverse Gaussian distribution. *Stochastic Processes and their Applications*. Elsevier; 1978; 7: 49–54.
61. Cutsuridis V. Behavioural and computational varieties of response inhibition in eye movements. *Philos Trans R Soc Lond, B, Biol Sci*. 2017; 372.
62. Logan GD, Van Zandt T, Verbruggen F, Wagenmakers EJ. On the ability to inhibit thought and action: general and special theories of an act of control. *Psychol Rev*. 2014; 121: 66–95. <https://doi.org/10.1037/a0035230> PMID: 24490789
63. Cutsuridis V, Smyrnis N, Evdokimidis I, Perantonis S. A neural network model of decision making in an antisaccade task by the superior colliculus. *Neural Networks*. 2007; 20: 690–704. <https://doi.org/10.1016/j.neunet.2007.01.004> PMID: 17446043
64. Cutsuridis V, Kumari V, Ettinger U. Antisaccade performance in schizophrenia: a neural model of decision making in the superior colliculus. *Front Neurosci*. 2014; 8: 13. <https://doi.org/10.3389/fnins.2014.00013> PMID: 24574953
65. Cutsuridis V. Neural competition via lateral inhibition between decision processes and not a STOP signal accounts for the antisaccade performance in healthy and schizophrenia subjects. *Front Neurosci*. 2015; 9: 5. <https://doi.org/10.3389/fnins.2015.00005> PMID: 25688183
66. Brown JW, Bullock D, Grossberg S. How laminar frontal cortex and basal ganglia circuits interact to control planned and reactive saccades. *Neural Netw*. 2004; 17: 471–510. <https://doi.org/10.1016/j.neunet.2003.08.006> PMID: 15109680
67. Heinzle J, Hepp K, Martin KA. A microcircuit model of the frontal eye fields. *J Neurosci*. 2007; 27: 9341–9353. <https://doi.org/10.1523/JNEUROSCI.0974-07.2007> PMID: 17728448
68. Wiecki TV, Frank MJ. A computational model of inhibitory control in frontal cortex and basal ganglia. *Psychol Rev*. 2013; 120: 329–355. <https://doi.org/10.1037/a0031542> PMID: 23586447
69. Carpenter R, Noorani I. Movement suppression: brain mechanisms for stopping and stillness. *Philos Trans R Soc Lond, B, Biol Sci*. 2017; 372.
70. Boucher L, Palmeri TJ, Logan GD, Schall JD. Inhibitory control in mind and brain: an interactive race model of countermanding saccades. *Psychol Rev*. 2007; 114: 376–397. <https://doi.org/10.1037/0033-295X.114.2.376> PMID: 17500631
71. Schmidt R, Berke JD. A Pause-then-Cancel model of stopping: evidence from basal ganglia neurophysiology. *Philos Trans R Soc Lond, B, Biol Sci*. 2017; 372.
72. Bissett PG. The countermanding task revisited: mimicry of race models. *J Neurosci*. 2013; 33: 12150–12151. <https://doi.org/10.1523/JNEUROSCI.2091-13.2013> PMID: 23884923
73. Schall JD, Palmeri TJ, Logan GD. Models of inhibitory control. *Philos Trans R Soc Lond, B, Biol Sci*. 2017; 372.

74. Schmidt R, Leventhal DK, Mallet N, Chen F, Berke JD. Canceling actions involves a race between basal ganglia pathways. *Nat Neurosci*. 2013; 16: 1118–1124. <https://doi.org/10.1038/nn.3456> PMID: [23852117](https://pubmed.ncbi.nlm.nih.gov/23852117/)
75. Stuphorn V, Schall JD. Executive control of countermanding saccades by the supplementary eye field. *Nat Neurosci*. 2006; 9: 925–931. <https://doi.org/10.1038/nn1714> PMID: [16732274](https://pubmed.ncbi.nlm.nih.gov/16732274/)
76. Pouget P, Murthy A, Stuphorn V. Cortical control and performance monitoring of interrupting and redirecting movements. *Philos Trans R Soc Lond, B, Biol Sci*. 2017; 372.
77. Reuter B, Rakusan L, Kathmanna N. Poor antisaccade performance in schizophrenia: an inhibition deficit? *Psychiatry Res*. 2005; 135: 1–10. <https://doi.org/10.1016/j.psychres.2004.12.006> PMID: [15893384](https://pubmed.ncbi.nlm.nih.gov/15893384/)
78. Reuter B, Jager M, Bottlender R, Kathmann N. Impaired action control in schizophrenia: the role of volitional saccade initiation. *Neuropsychologia*. 2007; 45: 1840–1848. <https://doi.org/10.1016/j.neuropsychologia.2006.12.006> PMID: [17258779](https://pubmed.ncbi.nlm.nih.gov/17258779/)
79. Coe BC, Munoz DP. Mechanisms of saccade suppression revealed in the anti-saccade task. *Philos Trans R Soc Lond, B, Biol Sci*. 2017; 372.
80. Hakvoort Schwerdtfeger RM, Alahyane N, Brien DC, Coe BC, Stroman PW, Munoz DP. Preparatory neural networks are impaired in adults with attention-deficit/hyperactivity disorder during the antisaccade task. *Neuroimage Clin*. 2012; 2: 63–78. <https://doi.org/10.1016/j.nicl.2012.10.006> PMID: [24179760](https://pubmed.ncbi.nlm.nih.gov/24179760/)
81. Cameron IG, Pari G, Alahyane N, Brien DC, Coe BC, Stroman PW, et al. Impaired executive function signals in motor brain regions in Parkinson's disease. *Neuroimage*. 2012; 60: 1156–1170. <https://doi.org/10.1016/j.neuroimage.2012.01.057> PMID: [22270353](https://pubmed.ncbi.nlm.nih.gov/22270353/)
82. Witiuk K, Fernandez-Ruiz J, McKee R, Alahyane N, Coe BC, Melanson M, et al. Cognitive deterioration and functional compensation in ALS measured with fMRI using an inhibitory task. *J Neurosci*. 2014; 34: 14260–14271. <https://doi.org/10.1523/JNEUROSCI.1111-14.2014> PMID: [25339740](https://pubmed.ncbi.nlm.nih.gov/25339740/)
83. Remijnse PL, van den Heuvel OA, Nielen MM, Vriend C, Hendriks GJ, Hoogendijk WJ, et al. Cognitive inflexibility in obsessive-compulsive disorder and major depression is associated with distinct neural correlates. *PLoS ONE*. 2013; 8: e59600. <https://doi.org/10.1371/journal.pone.0059600> PMID: [23637737](https://pubmed.ncbi.nlm.nih.gov/23637737/)